UNIVERSITY OF JYVÄSKYLÄ
Department of Chemistry

Supramolecular systems based on gold(I) derivatives. Molecular recognition of L-glutamine and polyQ.

Master's thesis
University of Jyväskylä
Department of Chemistry
Laboratory of Organic Chemistry
6th August 2017

Noora Svahn

ABSTRACT

The study of new organometallic complexes possessing interesting luminescent properties that stem from the 4-ethynylaniline ligand with a contribution of phosphane unit and Au···Au interactions, have been employed in molecular recognition of L-glutamine and polyglutamine. Weak intermolecular interactions have been found to result in fibrillary and spherical shapes of aggregates with different morphology in the presence of the guest molecules. The binding mode in the host-guest system shows different emission behaviour depending on the guest molecule. Furthermore, thermodynamic functions of the self-assembly of [Au(4ethynyl-aniline)(PTA)] was investigated through variable concentration and temperature NMR studies. The linear gold(I) complexes aggregate into long organized fibres *via* an isodesmic polymerisation mechanism and regardless of the previous studies with related complex the process has been observed to be entropically driven.

Index Terms– Aggregation, Aurophilic Interaction, Gold(I), Luminescence, Molecular Recognition, PEG.

TIIVISTELMÄ

L-glutamiinin ja polyglutamiinin molekyylintunnistuksessa käytettyjen uusien organometallikompleksien mielenkiintoiset luminesoivat ominaisuudet ovat peräisin 4-etynyylianiliiniligandista ja fosfaaniyksiköstä sekä molekyylien välisistä Au···Au vuorovaikutuksista. Heikkojen intermolekulaaristen vuorovaikutusten on havaittu johtavan kuitu- ja pallomaisten muotojen morfologisiin muutoksiin vierasmolekyylien läsnä ollessa. Muodostunut isäntä-vieras -kompleksi tuottaa erilaisen emission vierasmolekyylistä riippuen. Lisäksi [Au(4-etynyylianiliini)(PTA)]:n itsejärjestäytymisen termodynaamisia funktioita tutkittiin eri pitoisuuksissa ja lämpötiloissa NMR mittausten avulla. Nämä lineaariset kulta(I) -kompleksit järjestäytyvät pitkiksi kuiduiksi isodesmisen polymerisaatiomekanismin avulla, jonka on havaittu olevan entropian ajama riippumatta aikaisemmista tutkimuksista saman kaltaisilla komplekseilla.

Hakutermit– Aggregaatio, Aurofiilinen vuorovaikutus, Kulta(I), Luminesenssi, Molekyylintunnistus, PEG.

PREFACE

The experimental and the literature part of the Master's thesis were done during the time period of September 2016–June 2017 and the defending of the Master's thesis was successfully completed on 5th of July 2017 at the University of Barcelona in Spain. The literature search was done utilizing Web of Science, SciFinder, Reaxys and Google Scholar.

N. S. Author would like to express the greatest gratitude to Dr. Laura Rodríguez who supervised this Master's thesis work and for giving an opportunity to work among her research group. Furthermore, the author wishes to thank the colleagues whom been part of the exchange year at University of Barcelona and everyone else who has contributed to the author's chemistry studies throughout the past years. The author is also grateful for the financial support of Erasmus exchange program. Moreover, Academy Professor Kari Rissanen is acknowledged for the chance to carry out the Master's thesis abroad during the author's Erasmus exchange year.

CONTENTS

ABBREVIATIONS

ACN	Acetonitrile
DAPTA	3,7-Diacetyl-1,3,7-triaza-5-phosphabicyclo[3.3.1]nonane
DCM	Dichloromethane
DEE	Diethyl ether
DMSO	Dimethyl sulfoxide
HD	Huntington's disease
HOMO	Highest occupied molecular orbital
IL	Intraligand
ISC	Intersystem Crossing
LMWG	Low molecular weight gelator
LUMO	Lowest unoccupied molecular orbital
MeOH	Methanol
OM	Optical microscopy
PEG	Polyethylene glycol
PTA	1,3,5-Triaza-7-phosphaadamantane
RT	Room temperature
TBAH	Tetrabutylammonium hydroxide
TBAHS	Tetrabutylammonium hydrogen sulfate
THF	Tetrahydrofuran
THT	Tetrahydrothiophene

1. INTRODUCTION

Gold has been highly valued and desired metal for its durability, inertness and popularity as an investment option since the ancient times. Among organometallic chemists, gold has attracted remarkable interest due to its ability to establish metal···metal interactions, known as aurophilicity[1], [2]. Stabilizing Au···Au contacts (~3.0–3.5 Å maximum distance) associated with bond energy of standard hydrogen bond (5–10 kcal/mol)[3], can lead to intriguing supramolecular assemblies together with other non-covalent interactions including *e.g.* hydrogen bonding, π-π stacking and Van der Waals forces.

In particular, low molecular weight gold(I) complexes have a tendency to form supramolecular gels (LMWG) by aggregating[4]–[6]. However, the solvent plays an important role in the gelation process and together with the intermolecular interactions can lead to different polymeric structures such as fibers, micelles, rods, spherical and helical shapes among others[7].

LMWGs are termed as organogels when the fluid component is organic solvent and hydrogels when the molecules immobilize in water. In case of organogels, the main force for aggregation is commonly believed to be hydrogen bonding whereas in water hydrophobic interactions dominate[8]. Furthermore, the concentration of the monomers, chemical structure of the ligands and the strength of the non-covalent interactions will all affect on the association constant and therefore aggregation of the metallogels. Thus, the gelation properties and morphologies of LMWGs can be readily modified by rational design of the coordinating ligands in the organometallic system[9], [10].

The presence of Au···Au interaction in linear gold(I) complexes are fascinating not only for their stabilizing influence on LMWGs but due to their rich photophysical properties. The presence of heavy gold centre in mononuclear gold(I) complexes can lower the gap between HOMO (highest occupied molecular orbital) and LUMO (lowest unoccupied molecular orbital) and thus result in long-lived luminescence.

Research interest in novel gold(I) complexes containing alkynyl units has grown during the past 20 years due to their potential suitability for future applications in diverse fields such as molecular electronics, environmental science, therapeutics, catalysis and material science[11]. More recently, the interest in gelating gold(I)-alkynyl complexes from the biological point of view has grown and the results are rather promising[12]. In addition, our group has reported on anticancer properties of gold(I) complexes where the metal ion is coordinated with water soluble phosphane ligands PTA(1,3,5-Triaza-7-phosphaadamantane) or DAPTA(3,7-Diacetyl-1,3,7-triaza-5-phosphabicyclo[3.3.1]nonane) and alkynyl ligand[13], [14]. As a result, we have extented the studies on neurodegenerative diseases. The interest of this work was particularly in polyglutamine (polyQ, Chart 1), that is related to diseases that are a group of nine inherited neurodegenerative disorders, including Huntington's disease (HD), which is caused by expansion of cytosine-adenine-guanine (CAG) repeat in DNA coding for a long polyQ tract in the particular proteins[15]–[17]. The disease pathway involves the mutant polyQ-containing protein aggregation that is associated with the toxicity. The formed mutant proteins gradually accumulate in nuclei, cytoplasm or extracellular space as in other neurodegenerative diseases as Alzheimer and Parkinson diseases. HD affects muscle coordination and cognitive abilities that lead to long-time physical weakening with depression and eventually to death. Currently, HD has no effective therapy and the approved treatment options can only relieve the disease symptoms.

These details have been the starting points of the work reported herein. Different kind of gold(I) complexes containing the general formula [Au(C≡C-org)(PR_3)] (org= 4-ethynylaniline and 6-ethynyl-1H-benzo[de]isoquinoline-1,3(2H)-dione; PR_3= PTA,

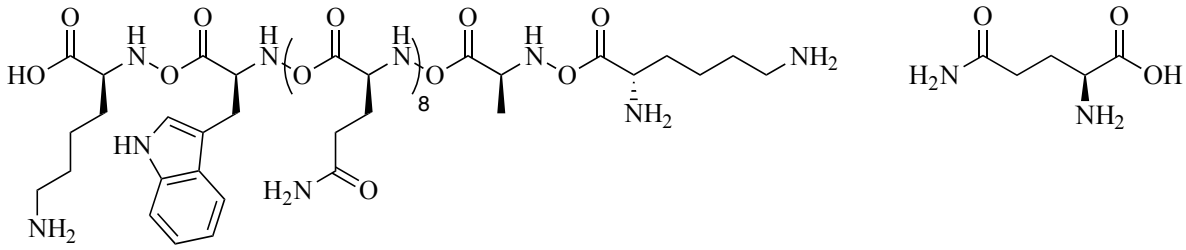

Chart 1. *Molecular structure of polyQ(left) and L-Glu(right).*

DAPTA, tri-1-naphthylphosphine) have been synthesized in order to investigate the molecular recognition of L-glutamine (L-Glu) and polyQ (Chart 1). Several spectroscopic techniques have been employed to address the binding mode of the gold(I) alkynyl compounds with L-Glu or polyQ. Furthermore, the synthesized complexes were characterized by Infrared (IR), proton and phosphorus Nuclear Magnetic Resonance (^{1}H and ^{31}P NMR) as well as with Electrospray Mass Spectrometry (ESI-MS).

In addition, the photophysical properties of the gold(I) compounds were examined with UV-vis spectrophoto- and spectrofluorimeter to attribute the self-assembly and presence of aurophilic interactions in solution. Moreover, the thermodynamic parameters responsible for the aggregation process were assayed with variable temperature and concentration ^{1}H and ^{31}P NMR experiments.

Furthermore, two different methods have been used to analyze the size of the synthesized compounds as well as the host-guest systems, including Dynamic Light Scattering (DLS) and Optical Microscopy. Finally, the synthesis of organic polyethylene glycol (PEG) ligand have been studied and assayed with several different reaction conditions. However, all the attempts to obtain PEG amide were unsuccessful. Nevertheless, the work will be continued with the successfully synthesized PEG nitrile.

2. EXPERIMENTAL PART

2.1. General Methods and Procedures

Reactions (when indicated) were carried out in high-purity N_2 atmosphere by using standard Schlenk techniques. Used dry solvents (DEE, Hexane and DCM) were from a Solvent Purification System (Innovative Technologies). MeOH and ACN were purged 30 min under N_2 flow prior to use. The commercial reagents diethylene glycol (Aldrich, ≥99%), acrylonitrile (Aldrich, 99%), 4-ethynylaniline (Aldrich, 97%), 1,3,5-triaza-7-phosphatricyclo[3.3.1.13.7]decane (PTA, Aldrich, 97%), 3,7-diacetyl-1,3,7-triaza-5-phosphabicyclo[3.3.1]nonane (DAPTA, Aldrich, 97%), tri-1-naphthylphosphine (Aldrich, 97%), tetrahydrothiophene (Merck, 98%), $HAuCl_4$ (Chambers Hispania S.A.), propargyl bromide (Aldrich, 80 % in toluene) were used as received. [AuCl(PTA)],[18] was

synthesized by Dr. Elisabet Aguiló (University of Barcelona) and 6-ethynyl-1H-benzo[de]isoquinoline-1,3(2H)-dione by Dr. Artur Moro (New University of Lisbon). ^{1}H and $^{31}P\{^{1}H\}$-NMR spectra were recorded in $CDCl_3$, MeOH-d_4, DMSO-d_6 and D_2O, which were purchased from Sigma Aldrich. The complexes Au(THT)Cl, [19] and [Au(4-ethynylaniline)]$_n$, [20] were prepared according to the existing literature.

2.1.1. Physical Measurements

NMR spectra were recorded using either a Varian Mercury 400 MHz or a Bruker 400 MHz Avance III spectrometer. ^{1}H chemical shifts are reported relative to tetramethylsilane (TMS) while ^{31}P chemical shifts are reported relative to 85% H_3PO_4 as an external standard. Electrospray Mass Spectra were recorded using a Fision VG Quatro spectrometer. Infrared spectroscopy was performed using a FT-IR 520 Nicolet spectrophotometer. Absorption spectra were recorded on a Varian Cary 100 Scan UV-spectrophotometer and emission spectra were recorded using a Horiba Jobin-Ybon SPEX Nanolog spectrofluorimeter. Dynamic light scattering measurements were carried out by using ZS 100 Nanoparticle Analyzer at 173° scattering angle at 25 ℃. Optical microscopy images were obtained with Leica ICC50 W. TLC was carried out with aluminum pre-coated silica gel 0.2 mm plates. Column chromatography was performed using Fluka silica gel (60 Å).

2.1.2. Titration Procedure

UV-Visible and fluorometric titrations were performed in H_2O (2.0×10^{-5} M) in the case of compounds **3** and **4** and in 1:1 THF:H_2O mixture (1.0×10^{-5} M) in the case of **5**. Titrations with L-glutamine were done as follows: small additions of L-glutamine (6.0×10^{-4} M) were introduced subsequently to a 3.0 ml portion of complex solution in a quartz cell using a micropipette. To reach the 1:1 equivalence, L-glutamine was added in 10×10 µl portions followed by 5×20 µl additions to reach 2:1 equivalence. Titrations with polyQ were performed as follows: a 3.0 ml portion of complex solution in a quartz cell was titrated by small additions of polyQ (2.8×10^{-4} M) in H_2O using a micropipette. To reach the 1:1 equivalence, polyQ was added in 10×2.6 µl portions followed by 5×36.6 µl additions to reach 2:1 equivalence. L-glutamine titrations were carried out for all **3**-**5** complex but polyQ only for **4** and **5**. The total added volume in L-glutamine titrations was 200 µl and in

polyQ 209 µl. In both cases after addition of the guest solution (L-glu or polyQ) in each step, the solutions were mixed thoroughly and then absorption spectra were recorded followed by emission and excitation spectra. In polyQ titrations all the spectra were recorded immediately and after 10 min of polyQ addition.

2.2. Syntheses

2.2.1. Synthesis of [AuCl(THT)] (1)

Tetrahydrothiophene (1.70 ml, 19.27 mmol) was added dropwise to a stirring yellow solution of $HAuCl_4$ (0.36 g, 15.77 mmol) in 1:6 EtOH:H_2O mixture Yellow solid precipitated immediately. After stirring for 30 min the precipitate was filtrated through glass frit and washed with EtOH (3×20 ml). White solid was dried under vacuum and gave 2.51 g (50%) yield.

^{1}H NMR (400 MHz, $CDCl_3$): δ_H 3.41 (br. d, *J*=68.3 Hz, 4H, S-C*H*$_2$-C) and 2.19 (br. d, *J*=70.4 Hz, 4H, C-C*H*$_2$-C) ppm. IR (KBr, ν_{max} cm^{-1}): ν(C-H) 2916 and ν(C-C) 1424.

2.2.2. Synthesis of [Au(C≡C-$C_6H_4NH_2$]$_n$ (2)

NEt_3 (0.54 ml, 3.87 mmol) and AuCl(THT) (0.70 g, 2.19 mmol) were added into a stirring solution of 4-ethynylaniline (0.26 g, 2.20 mmol) in DCM (35 ml) under N_2 atmosphere at rt. After stirring for 30 min the orange suspension was filtered, washed with DCM (3×15 ml) and dried under vacuum. Yield of the orange solid 0.63 g (92%).

IR (KBr, ν_{max} cm^{-1}): ν(N-H) 3363, 3202, ν(C≡C) 1994, ν(C=C) 1600 and ν(C-N) 1298.

2.2.3. Synthesis of [Au(4-ethynylaniline)(PTA)] (3)

PTA (50.5 mg, 0.32 mmol) was added into a stirring suspension of [Au(C≡C-$C_6H_4NH_2$]$_n$ (0.10 g, 0.32 mmol) in DCM (20 ml) under N_2 atmosphere at rt. The reaction mixture turned white after 10 min of stirring. The resulting suspension was concentrated in half volume after 2 h of stirring, hexane (17 ml) was added to favor precipitation and left in a fridge for several hours. The white solid was filtrated, washed with hexane (3 ml) and dried under vacuum. Purification of the solid was performed by stirring in 10:3.3

DCM:MeOH:ACN mixture. The suspension was concentrated, hexane (10 ml) added and left in a fridge for several hours. The filtrated and dried product gave a white solid in 95.3 mg (63%) yield.

^{1}H NMR (400 MHz, $CDCl_3$): δ_H 7.26 (dt, *J*=8.4, 2.4 Hz, 2H, H_β), 6.55 (dt, *J*=8.4, 2.4 Hz, 2H, H_α), 4.56, 4.45 (ABq, *J*=13.4 Hz, 6H, N-CH_2-N), 4.22 (s, 6H, N-CH_2-P) and 3.68 (br. s, 2H, NH_2) ppm. ^{31}P{^{1}H}-NMR ($CDCl_3$, 400 MHz): δ -49.4 (s, 1P) ppm. IR (KBr, ν_{max}cm^{-1}): ν(N-H) 3424, 3355 and ν(C≡C) 2102. ESI-MS *m/z* 471.10 ([M+H]$^+$, calc.: 471.10).

2.2.4. Synthesis of [Au(4-ethynylaniline)(DAPTA)] (4)

DAPTA (73.7 mg, 0.32 mmol) was added at once into a stirring suspension of [Au(C≡C-$C_6H_4NH_2$]$_n$ (0.10 g, 0.32 mmol) in DCM (20 ml) under N_2 atmosphere at rt. The reaction mixture turned clear yellow after stirring for 10 min. The resulting yellow suspension was concentrated after 2 h of stirring, hexane (17 ml) added in order to favor the precipitation and left in a fridge for several hours. The yellow solid was filtrated through cannula, washed with hexane (6 ml) and dried under vacuum. The yellow product was recrystallized from 5:1 DCM: MeOH mixture twice, concentrated, DEE (5 ml) added to precipitate the product and filtrated through cannula. Extra washing with DEE (50 ml) in glass frit did not give the pure product. Final purification by stirring in ACN (10 ml) for 1.5 h gave the pure product after concentrating, adding DEE (7 ml), keeping in a fridge for several hours, filtrating and washing with DEE (30 ml). The resulting yellow solid was dried under vacuum and gave 88.7 mg (51%) yield.

^{1}H NMR (400 MHz, $CDCl_3$): δ_H 7.27 (dt, *J*=7.7, 2.7 Hz, 2H, H_β), 6.56 (dt, *J*=8.5, 2.4 Hz, 2H, H_α), 5.79 (d, *J*=22.3 Hz, 1H, N-CH_2-N), 5.60 (dd, *J*=15.6, 7.0, 1H, P-CH_2-N), 4.95 (d, *J*=14.3 Hz, 1H, N-CH_2-N), 4.56–4.64 (m, 2H, N-CH_2-N and P-CH_2-N), 4.09 (dt, *J*=15.9, 3.0 Hz, 1H, P-CH_2-N), 4.04 (d, *J*=14.8 Hz, 1H, N-CH_2-N), 3.82 (s, 2H, P-CH_2-N), 3.71 (s, 2H, C-NH_2), 3.49 (dt, *J*=16.0, 4.0 Hz, 1H, P-CH_2-N), 2.10 (d, *J*=2.2 Hz, 6H, CO-CH_3) ppm. ^{31}P{^{1}H}-NMR ($CDCl_3$, 400 MHz): δ -22.5 (s, 1P) ppm. IR (KBr, ν_{max} cm^{-1}): ν(N-H) 3456, 3353 and ν(C≡C) 2099. ESI-MS *m/z* 543.12 ([M+H]$^+$, calc.: 543.12).

2.2.5. Synthesis of [Au(4-ethynylaniline)(tri-1-naphthylphosphine)] (5)

Tri-1-naphthylphosphine (0.13 g, 0.32 mmol) was added at once into a stirring suspension of $[Au(C\equiv C\text{-}C_6H_4NH_2]_n$ (0.10 g, 0.32 mmol) in DCM (20 ml) under N_2 atmosphere at rt. The solution turned pale yellow and turbid after 10 min of stirring. The resulting suspension was concentrated in half volume after stirring for 2 h, hexane (15 ml) added and left in a fridge for several hours. The pale yellow suspension was filtrated through cannula, washed with hexane (5 ml) and dried in vacuum. The crude product was stirred in DCM (15 ml) for 1 h, concentrated, DEE (7 ml) was added and left in a fridge for 1 day. The pale yellow solid was filtrated and dried in vacuum. Final purification by stirring in ACN (10 ml) for 1.5 h gave the pure product after concentrating, adding DEE (7 ml), keeping in a fridge for several hours, filtrating through glass frit and washing with DEE (30 ml). The resulting pale yellow solid was dried under vacuum and gave 0.13 g (56%) yield.

^{1}H NMR (400 MHz, $CDCl_3$): δ_H 8.82 (d, *J*=8.4 Hz, 3H, C-*H*), 7.99 (dd, *J*=29.5, 7.8 Hz, 6H, C-*H*), 7.54 (dt, *J*=25.5, 7.2 Hz, 6H, C-*H*), 7.31 (td, *J*=7.2, 2.0 Hz, 6H, C-*H*), 7.22 (dt, *J*=8.5, 2.4 Hz, 2H, H_β), 6.50 (dt, *J*=8.4, 2.4 Hz, 2H, H_α), 3.61 (s, 2H, C-NH_2) ppm. ^{31}P{^{1}H}-NMR ($CDCl_3$, 400 MHz): δ 22.5 (s, 1P) ppm. IR (KBr, ν_{max} cm^{-1}): ν(N-H) 3451, 3354 and ν(C≡C) 2107. ESI-MS *m/z* 726.16 ($[M+H]^+$, calc.: 726.16).

2.2.6. Synthesis of potassium 4-(diphenylphosphanyl)benzoate (8a)

4-(Diphenylphosphanyl)benzoate (70.9 mg, 0.23 mmol) was treated with KOH (16.1 mg, 0.29 mmol) in methanol under N_2 atmosphere to produce potassium 4-(diphenylphosphanyl)benzoate. After stirring for 1.5 h at rt the clear solution was concentrated till dryness. Resulting white solid was diluted in DEE by sonication, filtrated and dried under vacuum, which gave $(C_6H_5)_2PC_6H_4CO_2K$ in 66.7 mg (84%) yield.

^{1}H NMR (400 MHz, $CDCl_3$): δ_H7.47 (d, *J*=7.6 Hz, 2H, $HOOC_2$-C*H*), 7.11–7.17 (m, 10H, C-*H*), 6.86 (t, *J*=7.5 Hz, 2H, PC-C*H*) ppm. ^{31}P{^{1}H}-NMR ($CDCl_3$, 400 MHz): δ -6.2 (s, 1P) ppm. IR (KBr, ν_{max} cm^{-1}): ν(COOK) 1587, 1394. ESI-MS *m/z* 305.07 ($[M-K]^-$, calc.: 305.07).

2.2.7. Synthesis of [Au(6-ethynyl-1H-benzo[de]isoquinoline-1,3(2H)-dione)(PTA)] (10)

Previously synthesized ligand 6-ethynyl-1H-benzo[de]isoquinoline-1,3(2H)-dione (14.0 mg, 0.063 mmol), was dissolved in MeOH (5 ml) at rt under N_2 atmosphere and KOH (6.5 mg, 1.12 mmol) was added to deprotonate the alkynyl proton. After stirring for 30 min a solution of [AuCl(PTA)] (24.7 mg, 0.063 mmol) in DCM (5 ml) was added at once and the solution turned from clear brown to turbid yellow. After stirring for 22 h the reaction mixture was concentrated, DEE (10 ml) added to initiate the precipitation and left in a fridge for 2 h. Dark orange suspension was filtrated, washed with DEE (20 ml) and dried under vacuum to give dark orange solid in 27.5 mg (76 %) yield.

^{1}H NMR (400 MHz, DMSO): δ_H 11.67 (br. s, 1H, N-*H*), 8.57 (dd, *J*=73.4, 8.2 Hz, 1H, C-*H*), 8.28 (dd, *J*=24.6, 6.3 Hz, 1H, C-*H*), 8.14 (dd, *J*=22.2, 7.4 Hz, 1H, C-*H*), 7.76 (dt, *J*=22.6, 7.0 Hz, 1H, C-*H*), 7.62 (t, *J*=8.0 Hz, 1H, C-*H*), 4.63, 4.31 (ABq, *J*=12.8 Hz, 6H, N-C*H*$_2$-N) and 4.28 (s, 6H, N-C*H*$_2$-P) ppm. ^{31}P{^{1}H}-NMR (DMSO, 400 MHz): δ -12.0 (s, 1P) ppm. IR (KBr, ν_{max} cm^{-1}): ν(N-H) 3403, ν(C≡C) 2091 and ν(C=O) 1682. ESI-MS *m/z* 575.10 ([M+H]$^+$ calc.: 575.09).

2.2.8. Synthesis of 3-(2-(2-hydroxyethoxy)ethoxy)propanenitrile (11)

Acrylonitrile (4.32 ml, 65.96 mmol) was added to a stirring solution of diethylene glycol (6.27 ml, 65.95 mmol) and KOH (63.1 mg, 1.12 mmol) at rt. After stirring for 1.5 h the reaction was quenched with a few drops of HCl (5 mol/l). Unreacted acrylonitrile and H_2O were removed under reduced pressure. The residue was dissolved in DCM, filtrated through celite and concentrated under vacuum. The crude mixture was purified in column chromatography (5 % MeOH in DCM) to give 3-(2-(2-hydroxyethoxy)ethoxy)propanenitrile as a yellow oil in 3.34 g (35 %) yield.

^{1}H NMR (400 MHz, $CDCl_3$): δ_H 3.74–3.77 (m, 2H, O-C*H*$_2$), 3.73 (t, 2H, *J*=6.4 Hz, O-C*H*$_2$), 3.69 (s, 4H, O-C*H*$_2$), 3.61–3.63 (m, 2H, O-C*H*$_2$) and 2.63 (t, 2H, *J*=6.4, NC-C*H*$_2$) ppm. ^{13}C NMR (100 MHz, $CDCl_3$): δ_C 117.87 (1C, C≡N), 72.53, 70.68, 70.22, 65.83,

61.67 ppm. IR (KBr, ν_{max} cm^{-1}): ν(O−H) 3422, ν(C−H) 2878, ν(C≡N) 2251 and ν(C−O) 1114. ESI-MS *m/z* 160.10 ([M+H]$^+$, calc.: 160.10).

3. RESULTS AND DISCUSSION

3.1. Synthesis and Characterization

3.1.1. Synthesis of [Au(4-ethynylaniline)(PR_3)] (PR_3= PTA (3), DAPTA (4), tri-1-naphthylphosphine(5))

Complexes **3**–**5** have been synthesized by reacting the neutral oligomer [Au(C≡C-$C_6H_4NH_2$]$_n$ (**2**) with corresponding tertiary phosphanes PR_3 (R= PTA, DAPTA, tri-1-naphthylphosphine) in DCM for 2 h (Scheme 1). The oligomeric starting material is insoluble in DCM but becomes soluble when the phosphane ligand is added into the reaction mixture. In case of PTA and tri-1-naphthylphosphine the reaction took place in 10 min by forming white suspension while DAPTA caused an instant disappearance of the initial orange suspension and formed a clear yellow solution. Resulting suspensions and solution were concentrated and hexane added to obtain the desired products. Unreacted 4-ethynylaniline was removed by addition of ACN and by washing the solid products several times with DEE.

Products **3**–**5** were obtained as yellow solids in moderate yields (51–63 %) whose purity

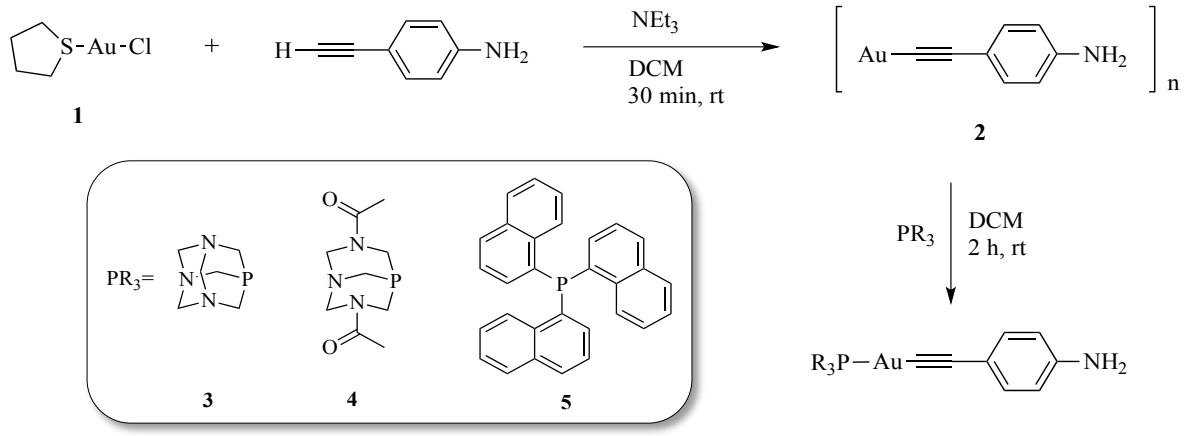

Scheme 1. *Synthesis of [Au(4-ethynylaniline)(PR_3)]* ***3***–***5***.

was determined by ^{1}H and ^{31}P NMR, IR and ESI-MS. IR spectra of products **3-5** show sharp peak at 2103 and 2107 cm^{-1} assigned to C≡C stretching. Both IR and ^{1}H NMR of **3-5** shows the disappearance of terminal alkynyl proton, which indicates of successful coordination to gold(I) atom.

^{1}H NMR spectrum of **3** shows the characteristic pattern of PTA protons; AB quartet at 4.56 and 4.45 ppm and a singlet at 4.22 ppm. Two triplets arising from the aniline ligand are seen at 7.26 and 6.55 ppm. The ^{1}H NMR spectrum of **4** shows classical resonances of DAPTA protons. Due to the non-symmetry of the ligand, the P-CH_2-N and the N-CH_2-N signals appear as five and four resonances respectively. A doublet arising from the protons at methyl groups in the acetyl group is seen at 2.10 ppm, which integrates as six protons.

The ^{1}H NMR spectrum of **5** shows doublet (8.82 ppm), doublet of doublets (7.99 ppm), doublet of triplets (7.54 ppm) and triplet of doublets (7.31 ppm) that can be assigned to the three naphthalene substituents. An upfield shift of proton signals is observed compared to the free ligand due to the coordination of the tri-1-naphthalynephosphine to the gold(I) alkynyl moiety. The protons of the amine group give a broad singlet at 3.68, 3.71 and 3.61 ppm in **3**–**5** ^{1}H NMR respectively. ^{31}P NMR shows one signal at -49.4 (**3**), -22.5 (**4**) and 22.5 (**5**) ppm downfield shifted compared to the free phosphane -98.0 (PTA)[21], -81.1 (DAPTA)[22], -33.1 ppm (tri-1-naphthalynephosphine), which indicates a successful coordination to the gold(I) atom. ESI-MS(+) spectrometry shows molecular peak ($[M+H]^{+}$) for all **3**–**5** complexes.

In addition, oligomer $[Au(C{\equiv}C\text{-}C_6H_4NH_2]_n$ (**2**) was complexed with two other phosphane ligands; 4-(diphenylphosphanyl)benzoic acid and 3-(diphenylphosphanyl)propanoic acid (Scheme S1). However, the compounds **6** and **7** could not be fully characterized due to a high impurity despite several purification procedures. Furthermore, the integration of proton signals in ^{1}H NMR did not match with the alleged products. Moreover, the aromatic protons of the phosphane ligands were shifted downfield in **6** and **7** as well as the splitting pattern of the same protons became non recognizable even though the ^{1}H NMR were measured in different solvents ($CDCl_3$, MeOH–d_4 and DMSO–d_6).

Based on the literature[23], [24], the oxygen of the both phosphane ligands could also coordinate with gold(I) and lead to a mixture of two different structures. In addition, the yellow solid of the synthesized **6** included some brown precipitate, which could be derived from reduced gold(I).

3.1.2. Synthesis of Potassium 4-(diphenylphosphanyl)benzoate (8a) and Anionic Organometallic Derivative of Chloro-Gold(I) (9a)

The synthesis of anionic organometallic complexes of 4-(diphenylphosphanyl)benzoic acid (**a**) and 3-(diphenylphosphanyl)propanoic acid (**b**) were assayed in order to obtain anionic chloro-gold(I) derivatives (Scheme S2) and then treat them with 4-ethynylaniline to obtain more water soluble alkynyl gold(I) complexes[25]. First, the acid group of benzylic group was neutralized with KOH. The reaction of 4-(diphenylphosphanyl)benzoic acid (**a**) with KOH gave $(C_6H_5)_2PC_6H_4CO_2K$, which was characterized by ^{1}H and ^{31}P NMR, IR and ESI-MS. Approximately 1.5 ppm downfield shifted signal in ^{31}P NMR, the absence of O-H and C=O vibration in the IR spectrum and the appearance of characteristic band at 1587 and 1394 cm^{-1}[26] are in accordance with the presence of COO^- ion (salts of carboxylic acid do not display carbonyl band due to symmetrical structure of COO^- ion, which is equally associated with the metal atom K^+). The reaction of 3-(diphenylphosphanyl)propanoic acid (**b**) with KOH did not give pure $C_{15}H_{15}O_2K$, which was proved by ^{31}P NMR showing two signals of phosphane.

The reaction of $(C_6H_5)_2PC_6H_4CO_2K$ with AuCl(THT) in DCM proceeded to give a mixture of products including decomposition of gold(I) complex (Scheme S2). Therefore, no pure anionic chloro-gold(I) complex could be isolated from these reactions.

3.1.3. Synthesis of [Au(6-ethynyl-1H-benzo[de]isoquinoline-1,3(2H)-dione)(PTA)] (10)

The first synthesis attempt of [Au(6-ethynyl-1H-benzo[de]isoquinoline-1,3(2H)-dione)(PTA)] (**10**) was performed by following the same method as described in the literature for compound **2**.[20] [AuCl(THT)] was reacted with deprotonated ligand, 6-ethynyl-1H-benzo[de]isoquinoline-1,3(2H)-dione, in DCM under N_2 atmosphere to form the following oligomer $[Au(6\text{-ethynyl-1H-benzo[de]isoquinoline-1,3(2H)-dione})]_n$. After stirring for 15 min, the orange solution turned dark brown and resulted in black precipitate that was gold nanoparticles. Another approach was performed successfully by reacting [AuCl(PTA)] with the corresponding ligand (Scheme 2). The first step in the synthetic route is the deprotonation of the terminal alkynyl proton with KOH in MeOH, which is then added into a solution of [AuCl(PTA)] in DCM under N_2 atmosphere. The ligand substitution takes place in 22 h at rt. The resulting yellow suspension was filtered through glass frit under ambient conditions and washed several times with DEE. Product **10** was obtained in good yield (76 %) whose purity was determined by ^{1}H and ^{31}P NMR, IR and ESI-MS.

The ^{1}H NMR spectrum of **10** shows five resonances of the aromatic protons at 7.62–8.57 ppm, which are upfield shifted compared to the starting compound. In addition, the proton at 7.76 ppm splits into doublet of triplets instead of a doublet and the proton at 7.62 ppm splits into a triplet instead of a doublet of doublets. These splitting and chemical shift changes within the aromatic protons might be due to the aggregation in DMSO-d_6, since the protons look more alike in $CDCl_3$. Moreover, the PTA protons aggregate in $CDCl_3$ by splitting into five resonances instead of the typical two; AB quartet and singlet. Thus, it seems that the compound aggregates in solvents with different polarity. The ^{31}P NMR shows one signal at -12.0 ppm, *ca*. 86 ppm downfield shifted compared to the free ligand. The IR spectrum shows a sharp peak at 2091 cm^{-1} assigned to the C≡C stretching. An absent alkynyl C−H peak at 3225 cm^{-1} indicated that the deprotonation has been successful

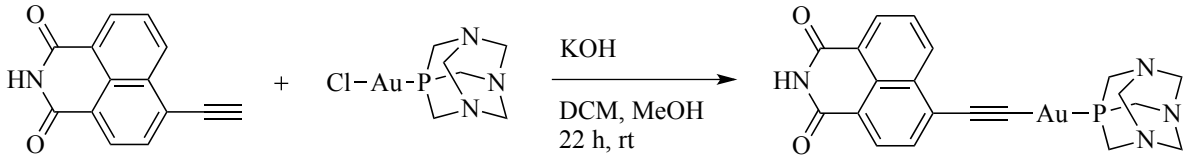

10

Scheme 2. *Synthesis of 6-ethynyl-1H-benzo[de]isoquinoline-1,3(2H)-dione derivative **10**.*

TABLE 1

Absorption and emission spectral data of the ligands, compounds **3** and **4** in H_2O and **5** in 1:1 THF:H_2O. λ_{exc}= 330 nm (**3**), 290 nm (**4**) 289 nm (**5**), 300 nm (Nap_3P), 270 nm[c] and 295 nm[b] (4-ethynylaniline). Emission in the solid state λ_{exc}= 425 nm (**3**) and 420 nm (**4**).

Compound	Absorption λ_{max}(nm) ($10^{-3}\varepsilon$ (M^{-1} cm^{-1}))	Emission λ_{max}(nm)	Solid State Emission λ_{max}(nm)
Nap_3P[b]	283 (35.8), 390 (1.9)	342	–
4-ethynylaniline	265 (28.3)[c], 277 (32.7)[b]	360[c], 352[b]	–
3	269 (16.4), 355 (3.8)	448	549
4	292 (19.5), 353 (3.4)	356, 459	549
5	298 (41.1), 381 (6.7)	342	[a]

[a] *Emission was too weak to record the maximum in solid state*
[b] *1:1 THF:H_2O mixture*
[c] *H_2O*

and the ligand has been coordinated to gold(I) atom. ESI-MS(+) spectrometry shows molecular peak for **10**.

3.2. Photophysical Characterization

The photophysical measurements were carried out in water as the main interest of this work was in biological applications. Since the complex **5** is not water soluble, the experiments were performed in 1:1 THF:H_2O mixture. The photophysical properties of complexes **3**–**5** depend on the nature of the chromophoric organic part of the molecule, in this case 4-ethynylaniline, and naphthalene of the tri-1-naphthylphosphine (Nap_3P) in the case of complex **5**. The electronic absorption and emission spectra were recorded for the compounds **3** and **4** at 2×10^{-5} M concentration and for compound **5** at 10^{-5} M concentration at rt. The results are summarized in Table 1.

The electronic absorption spectra of complexes **3**–**5** (Fig. 1) show intense high-energy bands in the range of 269–298 nm and low energy bands at *ca*. 353–381 nm. With reference to previous spectroscopic works on related alkynyl gold(I) complexes[27]–[31], the higher energy bands in complexes **3** and **4** are assigned as the $\pi-\pi^*$ transition of the 4-

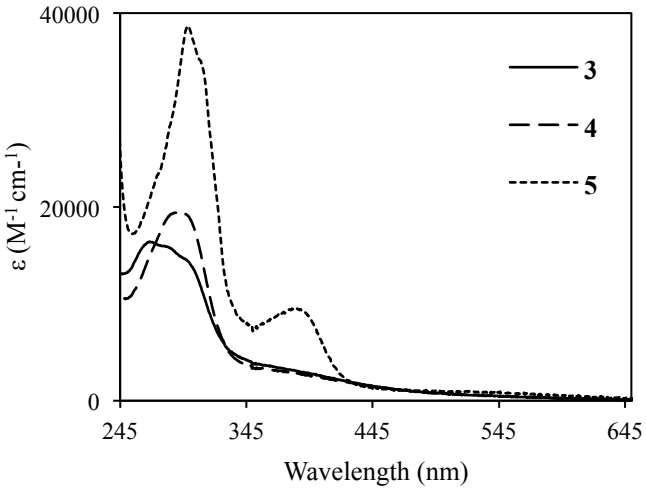

Fig. 1. *Absorption spectra of complexes **3** and **4** in H_2O and **5** in 1:1 THF:H_2O mixture.*

ethynylanilene ligand. This transition displays broadening and red shifting that can be due to aggregation of the complexes **3** and **4**.

The lower energy bands in complexes **3** and **4** at *ca*. 350 nm are assigned to a $\sigma^*_{Au-Au} \rightarrow \pi^*$ transition[28]. Previous research done with similar derivatives[30] suggest that the aurophilic (Au···Au) interactions are more easily established in water as it is a poor solvent and the monomers begin to aggregate by intermolecular interactions (mainly due to $\pi-\pi$ stacking and hydrogen bonding). Furthermore, ^{1}H NMR experiments of **3** support these findings as the 4-ethynylaniline protons show shifted populations in D_2O/DMSO–d_6 mixture (see below) that is an evidence of aggregation.

A comparison of the absorption band of **5** and its corresponding free Nap_3P ligand shows that the absorption maximum of **5** at 298 nm is red-shifted but retain similar vibronic structure that is typical of aromatic C-C vibrations. The absorption band at 298 nm is ascribed to the $\sigma \rightarrow \pi^*(Nap_3)$ transition[32]. The transition in free ligand involves the exciting of an electron from the lone pair orbital on P atom to an empty antibonding orbital of naphthyl group. Upon coordination of the phosphane ligand, the former lone electron pair now participates in sigma bonding to the Au atom. Thus, the σ electrons of the Au-P bond are available for donation to the low lying empty π^*(Nap) orbital. The electron density around the phosphorus atom is high due to the electron rich naphthyl substituents

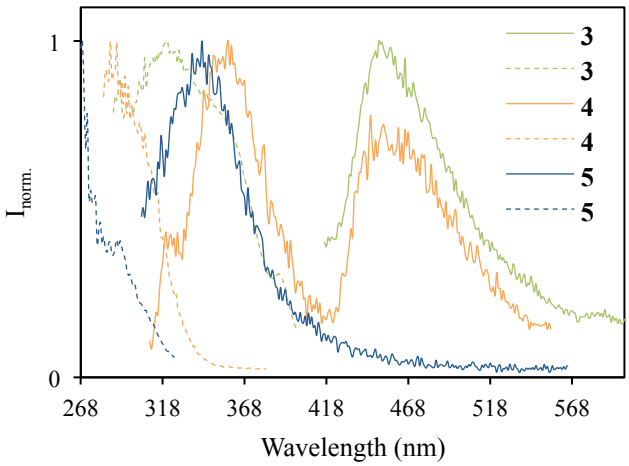

Fig. 2. *Normalized excitation (dashed line) and emission (solid line) spectra of* ***3*** *and* ***4*** *at* 2×10^{-5} *M concentration in* H_2O *and* ***5*** *at* 10^{-5} *M concentration in 1: THF:*H_2O *mixture at rt.*

and therefore, the absorption of the complex **5** is observed at lower energy compared to the free ligand.

Moreover, the naphthyl-groups in complex **5** adopt propeller geometry and possess steric bulky structure[33] that prevents the formation of Au···Au interactions. The low energy absorption band *ca*. 380 nm is observed to increase with higher concentrations but disappear in aged 10^{-5} M solution of complex **5**. This could be due to aggregate formation stemming from the interaction between naphthyl-groups in adjacent monomers. However, further research should be made to confirm the aggregate formation.

Upon excitation the sample at 330 nm (excitation spectra maximum) one emission band is observed for complex **3** centered at *ca*. 448 nm (Fig. 2) tentatively assigned to $^3[\pi–\pi^*$(alkynyl)] origin with contribution of gold atom[34]. Large Stokes shift usually indicate of radiative decay from the triplet state that results in phosphorescence[35]. The presence of heavy gold centre can boost the spin–orbit coupling of the system, which can subsequently enable the access to forbidden triplet excited states via intersystem crossing (ISC)[36].

In case of **4**, emission spectra recorded upon excitation of the lowest energy band shows two emission bands at 356 and 459 nm (Fig. 2). Excitation spectra collected at the emission maxima *ca*. 455 nm and 355 nm reproduce absorption of the 4-ethynylaniline, which

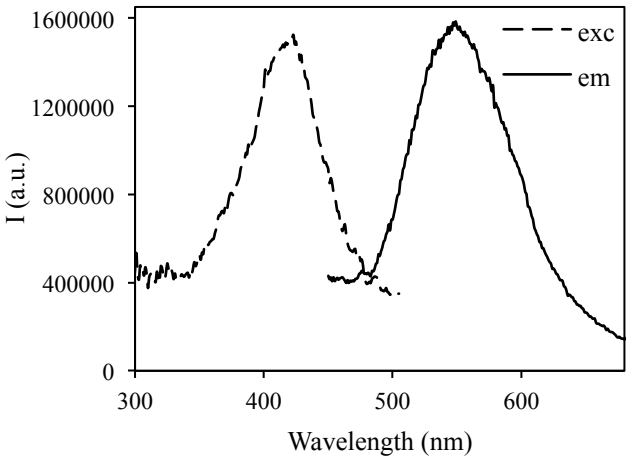

Fig. 3. *Solid state excitation (λ_{em}=535, dashed line) and emission (λ_{exc}=420, solid line) spectrum of **4** at rt.*

indicates that the origin of the emission is due to the 4-ethynylaniline moiety. These emissions have been assigned to metal perturbed ^{1}IL (intraligand) and ^{3}IL transitions, which is in agreement with the different Stokes' shifts[37], [38]. The emission maximum of **5** at ca. 342 nm originates from the 4-ethynylaniline as the excitation spectra collected at 345 nm produce a band with maximum at *ca*. 268 nm, thus being assigned to metal perturbed ^{1}IL transition.

Excitation of complexes **3** and **4** in the solid state gave rise to yellow emission at 550 nm at rt. The emission of **4** (Fig. 3) was approximately 3 fold more intense than the emission of **3.** When compared with the emission displayed in water at rt (λ_{em}=448-459 nm), the blue shift for the luminescence in solution can be attributed to larger structural changes that may occur in solution than in the rigid lattice of the solid. Referring to previous work in our group[39], polar solvents stabilize the ground state that can induce a blue shift of the absorption band.

3.3. Molecular Recognition

Molecular recognition studies of L-Glu and polyQ were carried out for complexes **3** and **4** in H_2O at 2.0×10^{-5} M concentration and only of L-Glu for **5** in 1:1 THF:H_2O mixture at 1.0×10^{-5} M concentration at rt. Electronic absorption and emission spectra were recorded for titrations of complexes **3**–**5** as described in the titration procedure in the experimental

section. ^{1}H and ^{31}P NMR studies were performed for **3** and **4** with L-Glu in 1:1 D_2O/DMSO–d_6 mixture.

3.3.1. L-Glutamine-binding Studies

The absorption bands in the range of 269–355 nm and emission bands at 448 nm of complex **3** show a drop in intensity upon addition of L-Glu (Fig. S1). The binding stoichiometry obtained by nonlinear regression does not show clear correlation between the host and the guest molecule. However, the slope has a marginal change at 1:1 stoichiometry and therefore it was chosen for the Dynamic Light Scattering (DLS) and ^{1}H and ^{31}P NMR studies.

^{1}H and ^{31}P NMR spectroscopy of **3** in the presence of 0.5, 1.0 and 1.5 eq. of L-Glu in 1:1 DMSO–d_6:D_2O mixture has been performed to analyze the binding form. The α-proton of L-Glu has an upfield shift when added into a solution of complex **3.** In addition, the resonance of the phosphorus in ^{31}P NMR shifts when different equivalents of L-Glu are added. Furthermore, in ^{1}H NMR spectrum, a *ca*. 0.002 ppm upfield shift is observed in the 4-ethynylaniline resonances and a small 0.01 ppm upfield shift in the case of PTA protons when L-Glu is added. Additionally, the resonance of the PTA protons do not shift further after adding 1.0 eq. of L-Glu, which could be indication that the binding stoichiometry is 1:1. According to these results, there is a weak interaction between the L-Glu and the complex **3** involving immediacy of the phosphorus and 4-ethynylaniline moieties as well as the α-proton of L-Glu.

Parallel molecular recognition experiments of L-Glu were carried out for complex **4** in H_2O. A similar trend has been observed in electronic absorption and emission spectra showing a drop in intensity upon addition of L-Glu (Fig. S2). The stoichiometric ratio of the host and the guest is seen to be 1:1 equivalence as well, since the slope decreases slightly at this point. The results show that the binding event mainly involves the DAPTA moiety as a modest, 0.02 ppm, upfield shift is observed for the acetyl protons in ^{1}H NMR of the complex **4** with 0.5, 1.0 and 1.5 eq. of L-Glu (Fig. S3). Furthermore, the resonance of the H_α proton of the L-Glu is shifted *ca* 0.01 ppm downfield with increasing L-Glu

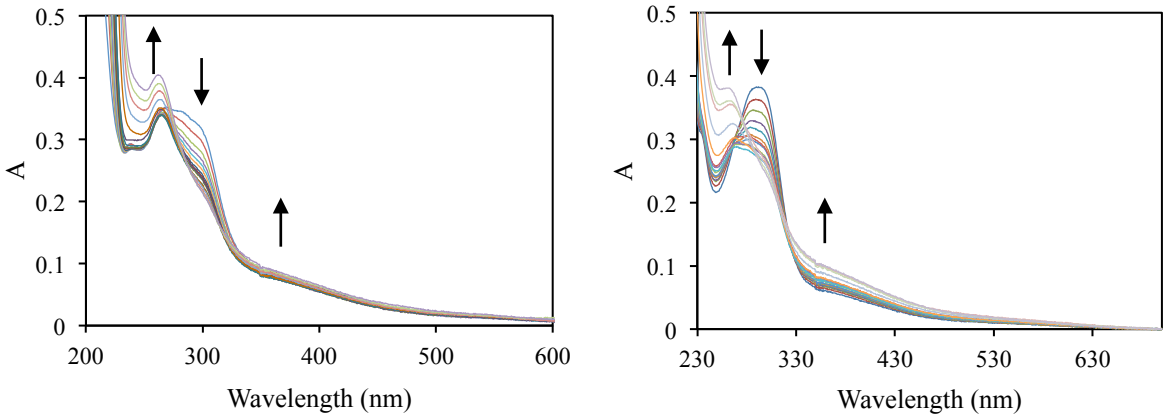

Fig. 4. *Absorption spectrum of **3** (left) and **4** (right) (2×10^{-5} M) in H_2O upon addition of polyQ (0→2 eq.) at rt. Arrows indicate increasing polyQ concentrations.*

concentration. Moreover, the ^{31}P NMR shows *ca*. 0.1 ppm upfield shift upon addition of L-Glu.

In the case of complex **5**, a decrease in absorption intensity at 298 and 381 nm is observed simultaneously with minor increase in emission intensity at 342 nm. Adversely, the emission at 419 nm upon excitation at 380 nm did not show any change in intensity during the titration of **5** with L-Glu (Fig S4).

3.3.2. PolyQ-binding Studies

The absorption spectrum of **3** and **4** shows a drop in intensity at *ca*. 300 nm with a simultaneous growth of higher energy band at *ca*. 265 nm and a low energy shoulder at *ca*. 360 nm upon addition of polyQ (Fig. 4) The 1:1 binding stoichiometry was observed by plotting the absorption at *ca*. 300 nm against the equivalence of the complex **3** and **4** with the polyQ (Fig. 5).

The absorption maximum is blue-shifted by ca. 35 nm when the polyQ concentration increases, clearly indicating the binding of the gold(I) complexes to the polyQ. According to literature[40], [41], such hypsochromic shifts can be attributed to a sandwich-type packing of the chromophores (H-aggregates) that in this case, are promoted by increasing concentration of polyQ.

The emission spectrum of **3** and **4** shows a blue-shifted, approximately six-fold higher intensity band at *ca*. 390 nm upon excitation at 330 nm (**3**) and 318 nm (**4**) (Fig. S5). According to the excitation spectrum collected at the emission maximum of the pure compounds at 450 nm (**3**) and 455 nm (**4**), the absorption at *ca*. 265 nm is responsible for the blue-shifted emission band at *ca*. 390 nm.

Further efforts will be made to extend the work to NMR studies to probe the binding mode. However, some assumption can be made about the interaction between the gold(I) complexes and polyQ. The binding by complexes **3** and **4** should be driven primarily by Van der Waals interactions and the hydrophobic effect as the gold(I) complexes are not highly water soluble and polyQ is known to aggregate in water at higher concentrations[42]. Furthermore, with the support of the UV-vis absorption and emission titrations, the binding mode of the complexes **3** and **4** with polyQ is believed to bring two gold centres into close proximity to turn on the higher energy emission based on Au···Au interactions. Enhance in intensity can also result from hydrophobic environment provided by polyQ that can protect the gold(I) complexes from quenching by water molecules[43], [44].

Absorption and emission spectra of **3** and **4** were recorded after 10 minutes of each polyQ addition. A drop in intensity was observed in each absorption spectra but the emission

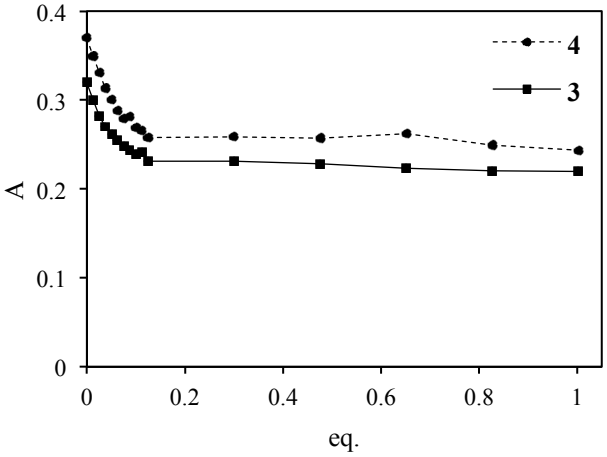

Fig. 5. *Plot of absorbance at 298 nm (**3**) and at 300 nm (**4**) as a function of equivalence of polyQ and complex **3** or **4**. Theoretical fit for the 1:1 binding.*

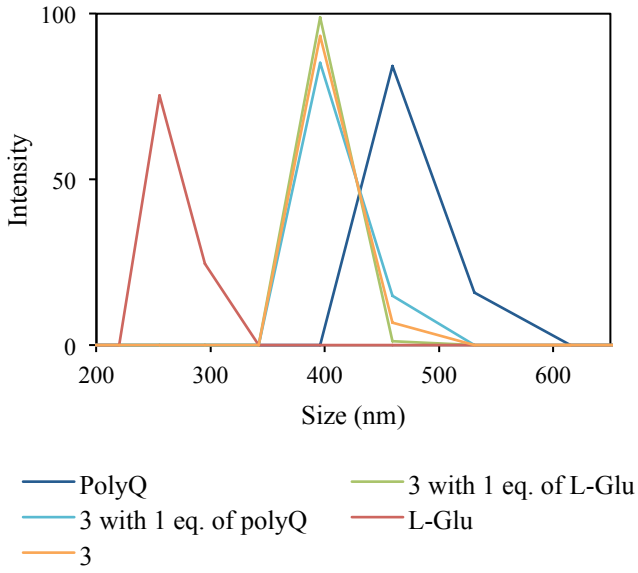

Fig. 6. *Size distribution of complex **3** at 2×10^{-5} M concentration with 1 eq. of polyQ and L-Glu and the guest molecules as well as the complex **3** alone.*

intensity remained at the same level as in the fresh samples, which suggests of instant interaction with the host and the guest molecule.

3.4. Dynamic Light Scattering (DLS)

Dynamic Light Scattering (DLS) measurements were performed to rationalize the aggregate's size resulting from molecular recognition studies. All the samples were prepared from fresh stock solutions in the same concentrations and solutions as in the titration studies. In the case of **3**, 1:1 eq. of complex with L-Glu and polyQ forms the same size of aggregates as the complex alone. It was observed that the size of polyQ aggregates alone in concentration 2.5×10^{-6} M is around 460 nm but when added to a solution of **3** (2.0×10^{-5} M) the size of the aggregates decreases to 400 nm. Same behavior was observed with L-glutamine at concentration 1.9×10^{-5} M when the aggregates increase in size to 400 nm in the presence of complex **3** (Fig. 6.). The results are in agreement with the titration studies, which show a clear interaction with both guest molecules.

The behavior is observed to be opposite in the case of **4**. The well-defined size of the complex increases from 250 nm to 350 nm when 1 eq. of L-Glu is added and to 450 nm when 1 eq. of polyQ is added (Fig. S6). Thus, it seems that polyQ-Au(I) complex

interactions align with the gold(I) complexes in the same way giving rise to similar size of aggregates. Same studies were carried out for complex **5** in 1:1 THF:H_2O mixture. When 1 eq. of L-glutamine is added to the 2.0×10^{-5} M solution of **5**, the size of the complex decreases from 390 nm to 100 nm (Fig. S6). The lower size of the resulting L-Glu-**5** adducts with respect to **3** and **4** may be due to the higher steric hindrance of the naphthyl phosphane that hinders the establishment of aurophilic contacts and formation of well-organized structures as observed in the previous cases. This is in agreement with the less effected emission spectra recorded in L-Glu titration studies.

However, in all cases high polydispercity index (PDI) was recorded, which could be due to larger aggregates in the solution. According to previous studies with gold(I) alkynyl complexes, the high PDI value could stem from the fact that these compounds form long 1D fibers and the DLS is modeled to determine spherical shape of aggregates.

3.5. Optical Microscopy

Optical microscopy (OM) analysis of the air-dried sample solutions of **3**–**5** indicates a clear formation of self-assembled structures. Long fibers up to few mm with smaller aggregates were observed in all cases. In addition optical microscopy analysis was performed with L-Glu and polyQ in same solutions as in DLS measurements. All of the samples polarize light, which is a clear evidence of very organized structures.

The presence of L-Glu and polyQ resulted in small spherical aggregates and large cross-linked fiber structures in case of complex **3** (Fig. S7). It seems that the fibers of compound **3** establish more complex and larger systems with the guest molecules. The smaller spherical aggregates seem to be similar size as the aggregates of the polyQ. However, polyQ also arrange into long fibers (∼2 mm) in addition to the spherical assemblies. L-Glu alone establishes spherical shape of aggregates together with longer fibers (<1.0 mm).

In case of **4**, cross-linked aggregates and long, up to few mm, fibers were formed in the presence of polyQ, while with L-Glu spherical and shorter fibers were found, which is in agreement with DLS studies (Fig. S8). The complex **4** alone established shorter fiber

assemblies. The presence of L-Glu organized small spherical aggregates of **5** in cross-linked fibers (Fig. S9), which is in agreement with the titration studies. However, longer fibers, up to 1 mm, were also found that were not detected in DLS possibly due to high PDI value and to the fact that OM images are resulting from dried samples, *i.e.* probably larger structures than in solution.

3.6. Impact of Temperature and Concentration on Aggregation

3.6.1. Variable Concentration NMR Studies

In order to investigate the self-assembly of complex **3**, several ^{1}H and ^{31}P NMR experiments were performed in 1:1 D_2O/DMSO–d_6 mixture at 4×10^{-4}–2×10^{-3} M concentrations and in pure DMSO–d_6 at 7×10^{-4}–5×10^{-3} M concentrations. Unfortunately, the low solubility in water prevented these studies in pure H_2O, which would have been a preferable solvent when taking into account the titration studies above.

^{1}H NMR spectra of compound **3** are moderately dependent on the concentration in 1:1 D_2O/DMSO–d_6 mixture. The α and β protons of 4-ethynylaniline resonate at two different frequencies at *ca*. $\delta(H_\beta)$ 7.15 and 7.00 ppm and $\delta(H_\alpha)$ 6.56 and 6.51 ppm. The latter group ($\delta(H_\beta)$ 7.00 ppm and $\delta(H_\alpha)$ 6.51 ppm) grows in intensity when the concentration is increased and thus they are ascribed to the aggregates (Fig. S10). On the other hand, different kind of aggregates are observed in pure DMSO–d_6 as four different aggregate groups are present in each concentration (Fig. S10). However, the integration of the aggregates increases inconsiderably with the increasing concentration, which annotates the distinct behavior in water and DMSO.

The monomer and aggregate resonances of 4-ethynylaniline present a small downfield shift with increasing concentration in both solvents indicating that the organic ligand is involved in the aggregation process.

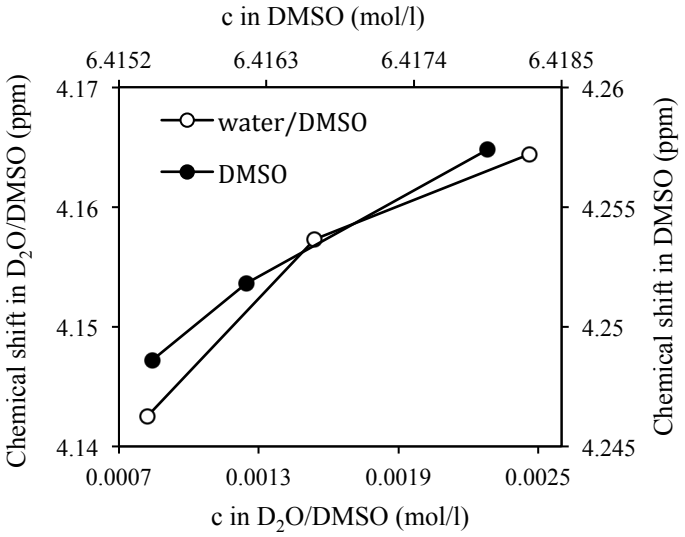

Fig 7. *Plot of PTA protons chemical shifts of* ***3*** *at 5×10^{-5} M concentration in DMSO–d_6 and H_2O/DMSO–d_6 mixture.*

The PTA protons (N-CH_2-P) are downfield shifted with increasing concentration in both solvents. However, the chemical shifts are larger in D_2O/DMSO–d_6 mixture than in pure DMSO–d_6 indicating that water enhances the aggregation of the water-soluble phosphane ligand (Fig. 7). Furthermore, in ^{31}P NMR there is approximately 0.3 ppm upfield shift in D_2O/DMSO–d_6 mixture and *ca*. 0.2 ppm upfield shift in DMSO–d_6 with increasing concentration due to the establishment of intermolecular interactions with adjacent molecules (Fig. S11). In addition, in D_2O/DMSO–d_6 mixture at higher concentrations another resonance of phosphorus is observed *ca*. 3 ppm downfield shifted from the major ^{31}P signal. This phenomenon was previously observed in similar studies performed with gold(I) alkynyl complexes[45] and is indicative of the presence of different type of aggregates at this concentration.

According to these experiments, the aggregation process is enhanced with increasing concentration in the presence of water. Moreover, 4-ethynylaniline and PTA protons display a small downfield shift with aggregation in used solvents. Two different environments are observed in water mixture while in pure DMSO aromatic protons are found to exist in several different environments.

3.6.2. Variable Temperature NMR Studies

The thermodynamic parameters responsible for the aggregates' formation were studied at 2×10^{-3} M concentration in D_2O/DMSO–d_6 mixture and at 5×10^{-3} M concentration in DMSO–d_6 between 298 and 338 K.

T-dependent measurements allow for accurate determination of thermodynamic parameters describing the aggregation process[46]–[49]. Based on the former studies with related neutral complexes[45], isodesmic model is used to describe the self-assembly of **3** instead of cooperative model, which involves two equilibrium constants: the initial, unfavorable formation of nucleation core followed by rapid expansion in the growing chain. The isodesmic model is based on an aggregation constant in which every monomer *M* addition to the growing chain is directed by the same equilibrium constant *K* exemplified in equations 1–3

$$M + M \overset{K}{\leftrightarrow} M_2 \quad (1)$$

$$M_2 + M \overset{K}{\leftrightarrow} M_3 \quad (2)$$

$$\ldots.$$

$$M_n + M \overset{K}{\leftrightarrow} M_{n+1} \quad (3)$$

However, all possible supramolecular aggregates in DMSO and D_2O/DMSO mixture must be considered. As discussed above, the gold(I) compounds do aggregate in DMSO but most likely form several different kinds of aggregates simultaneously. Nevertheless, the monomers of complex **3** are expected to aggregate via $\pi-\pi$ stacking and/or Au···Au interactions.

In D_2O/DMSO–d_6 mixture 4-ethynylaniline protons become more shielded with increasing temperature. More importantly, the integrations of the aggregate signals grow slightly with the temperature indicating that the increase in temperature moves the equilibrium towards the aggregates (Fig. S12). Opposite behavior can be observed in pure DMSO–d_6 as the aromatic protons shift downfield with increasing temperature, which is another evidence of distinct aggregates in DMSO and water.

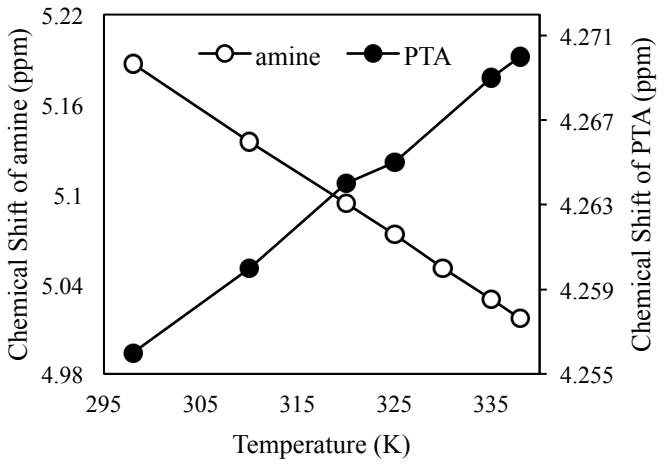

Fig. 8. *Plot of amine and PTA protons chemical shifts of* ***3*** *at* 5×10^{-3} *M concentration in DMSO–*d_6 *as a function of temperature.*

More significant effect caused by the rising temperature is observed in both solvents within the amine and PTA protons (Fig. 8). The amine protons shift upfield while the PTA protons downfield when the temperature increases. These data points out that both the aniline and the phosphorus ligand are involved in the aggregation process in both solvents. However, increasing temperature boost the aggregation process in the presence of water while in DMSO the molar fraction of the aggregates remain analogous when the temperature is raised.

To fit the temperature dependent ^{1}H NMR data to the equations 4 and 5 of isodesmic model, resulting from constant concentration c_0, in which *K* is the equilibrium constant and c_m the concentration of the monomer, molar fractions of monomer, x_m, and aggregates, x_a, can be obtained

$$x_m = \frac{c_m}{c_0} = \frac{1+2Kc_0-\sqrt{1+4Kc_0}}{2K^2c_0^2} \tag{4}$$

$$x_a = 1 - x_m = 1 - \frac{1+2Kc_0-\sqrt{1+4Kc_0}}{2K^2c_0^2} \tag{5}$$

In both equations the equilibrium constant *K* changes within the temperature according to equation (6)

$$K = e^{-\left(\frac{\Delta G}{RT}\right)} \quad (6)$$

where ΔG is the Gibbs free enrgy, R is the gas constant and T is the temperature. Since the temperature range of the experiments is small and ΔG is T-dependent, more suitable equation 7 is used to determine the thermodynamic constants of the self-assembly

$$K = e^{-\left[\left(\frac{\Delta H}{RT}\right)+\left(\frac{\Delta S}{R}\right)\right]} \quad (7)$$

where ΔH is the enthalpy and ΔS is the entropy. The results are shown in the Table 2. The thermodynamic parameters are very different in pure DMSO and in water mixture.

TABLE 2

Enthalpy, Entropy, Gibbs Free Energy and equilibrium constant K at 298 K for compound **3** at 2×10^{-3} M concentration in H_2O/DMSO and at 5×10^{-3} M concentration in DMSO.

	ΔH(kJ/mol)	ΔS (J/mol·K)	ΔG^{298} (kJ/mol)	K^{298}
3[a]	12.43	100.57	-17.54	1185.52
3[b]	28.32	97.15	-0.63	1.29

[a]H_2O/DMSO

[b]DMSO

The enthalpic penalty in DMSO could stem from the low tendency to aggregate in this solvent, as detected for the lower intensity aggregates' protons in ^{1}H NMR. In contrary, large ΔS indicates that the driving force for the aggregation is the entropy and it does not depend on the solvent rather the intermolecular interactions. The Gibbs free energy in water mixture is in the expected range for Au···Au contacts[45] and therefore we can conclude that aurophilic interactions enhance the aggregation process.

4. SELF-ASSEMBLY OF IONIC GOLD(I) COMPLEX

Similar variable temperature and concentration experiments were performed with previously synthesized complexes that were presented in the Practical Research of this Master program.

^{1}H NMR study at different temperatures and concentrations were performed in order to gain insight of formation of thermodynamic data of metallogelators formation. Previously synthesized ionic compound **13** $[Au(PTA)_2][Au(C{\equiv}CC_5H_4N)_2]$ (Fig. 9) was studied in different solvent compositions of H_2O/DMSO media. According to absorption and emission studies, increasing water composition effects positively to the aggregation process, which is observed as a blue-shift and band broadening. Furthermore, the aggregation seems to induce a fluorescence quenching.

4.1. Variable Concentration NMR Studies

In this work, complex **13** was studied only in DMSO–d_6 at 2×10^{-4}–8×10^{-4} M concentrations since the compound is not soluble in H_2O or H_2O/DMSO mixture at required concentration for liable NMR studies. The ^{1}H NMR spectra of **13** at different concentrations display pyridine protons at $\delta(H_\alpha)$ 8.44 ppm and two groups of $\delta(H_\beta)$ 7.21 and 7.33 ppm. The resonance of H_β at 7.21 ppm grows in intensity as well as in integration respect to the second resonance at 7.33 ppm when concentration is increased. Hence, the growing resonance is assigned to the aggregates and therefore, m

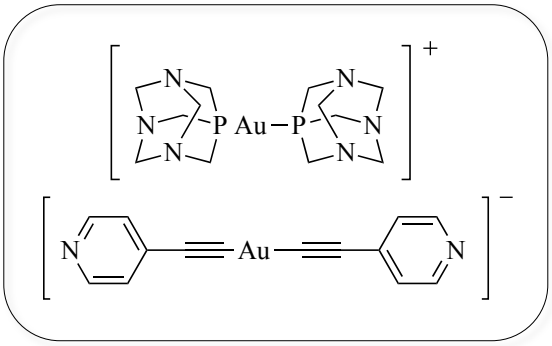

Fig. 9. *Molecular structure of $[Au(PTA)_2][Au(C{\equiv}CC_5H_4N)_2]$ (**13**).*

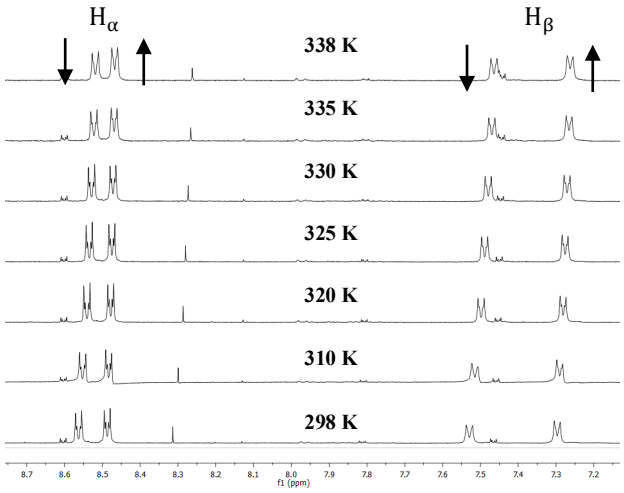

Fig. 10. *^{1}H NMR spectrum of **13** at 8×10^{-4} M concentration in DMSO–d_6 at different temperatures. Arrows indicate the variation in integration.*

olar fractions can be retrieved from integration of the NMR signals.

^{31}P NMR spectra recorded at the same concentrations range are in agreements with aggregation process. The resonance of phosphorus shifts upfield *ca*. 0.25 ppm with increasing concentration.

4.2. Variable Temperature NMR Studies

In order to determine the thermodynamic parameters of the self-assembly of **13**, temperature dependent ^{1}H NMR measurements were performed at 8×10^{-4} M concentration in DMSO–d_6.

The pyridine protons of **13** shift upfield with rising temperature (Fig. 10). Moreover, the integral of the aggregates (at lower frequency) grow moderately when the temperature is increased. The temperature dependent ^{1}H NMR data were fitted in equations 4 and 5 of isodesmic model described above. The results presented in Table 3 are revealing that the entropy rather than the enthalpy drives the aggregation process, which can arise from the release of water molecules upon interaction between molecules.

TABLE 3

Enthalpy, Entropy, Gibbs Free Energy and equilibrium constant K at 298 K for compound **13** at 8×10^{-4} M concentration in DMSO.

	ΔH(kJ/mol)	ΔS (J/mol·K)	ΔG^{298} (kJ/mol)	K^{298}
13	5.60	74.54	-16.61	815.03

As seen in Fig. 11, the increasing temperature favors the aggregation process of **13.** The contrary effect was previously observed in related neutral complex (Fig. S13) in which the aggregate formation is decreased with the rising T. The Gibbs free energy for a single step aggregation obtained from the VT ^{1}H NMR data is similar as for the neutral complex in water ($\Delta G = -25$ kJ/mol). These findings can conclude that the aggregation process might be due to the hydrophobic effects in addition to Van der Waals and aurophilic interactions.

5. LIGAND SYNTHESIS: POLYETHYLENE GLYCOL IN FOCUS

5.1. Synthesis of 3-(2-(2-hydroxyethoxy)ethoxy)propanenitrile (11)

The starting material **11** has been synthesized by conjugate addition of diethylene glycol (DEG) to acrylonitrile under ambient conditions (Scheme 3) by following similar approach previously described in the literature[50]. After stirring for 1.5 h, the reaction was completed by protonating the nitrile enolate with HCl. The pure product was obtained as

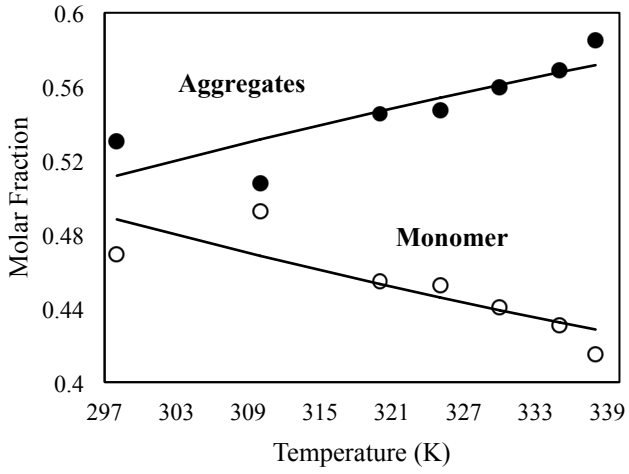

Fig 11. *Molar fractions of the aggregates (closed circles) and monomer (open circles) of complex **13** at 8×10^{-4} M concentration in DMSO. Fitting of the isodesmic model as a function of temperature.*

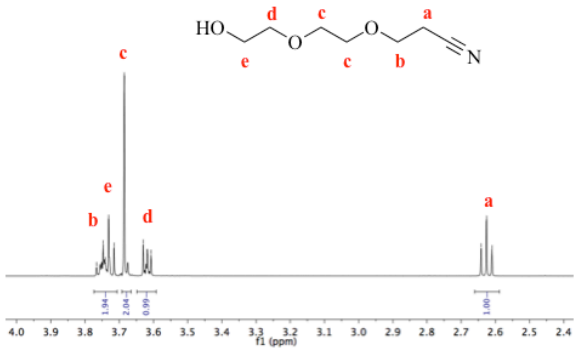

Fig. 12. *^{1}H NMR spectrum of **11** in $CDCl_3$. Assigned protons a–e in red.*

yellow oil after filtrating through celite and purification by column chromatography. The synthesis was not high-yielding (35 %) due to the formation of by-product, di-substituted polyethylene glycol (PEG) nitrile.

The purity of **11** was determined by ^{1}H and ^{13}C NMR, which revealed four distinct resonances associated with the twelve protons (Fig. 12) and seven carbons on the PEG-nitrile. IR showed distinctive stretching absorptions of nitrile, ether and O-H confirming the structure of **11**. Furthermore, ESI-MS(+) spectrometry shows molecular peak for **11**.

5.2. Hydrolysis of 3-(2-(2-hydroxyethoxy)ethoxy)propanenitrile (11)

The hydrolysis of crude **11** was attempted several times with $Pd(PPh_3)_4$ and tetrabutylammonium hydrogen sulfate (TBAHS) in alkaline conditions (Scheme 3) by following similar approach previously described in the literature[51]–[53]. However, no amide product (**12**) could be obtained, which is most likely due to the formation of volatile lactone. The used strategy may have given carboxylic acid as the major product. The proposed reaction mechanism is presented in Fig. S14. However, if the dimerization between the carboxylic acids in solution-state is weak, volatile lactones are expected. The secondary functional groups (C-O, CN and OH) may weaken the dimers of carboxylic acids and therefore the mixture becomes exposed for many possibilities.

The reaction was monitored *in situ* using IR and TLC (5 % MeOH in DCM), which showed streak for the product indicating that no polar compound (as the desired amide would be)

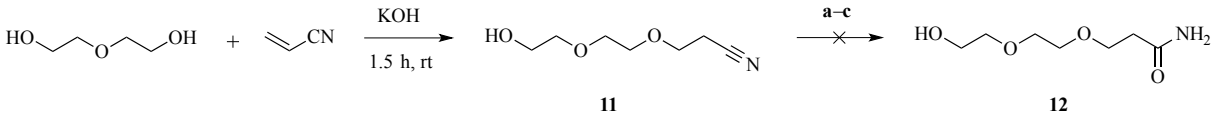

Scheme 3. *Synthesis of 3-(2-(2-hydroxyethoxy)ethoxy)propanenitrile **11** and different reaction conditions for the hydrolysis reaction of product **11**; **a:** $Pd(PPh_3)_4$ (3mol%), HCOOH, 1.5 h, rt, **b:** TBAHS (20 mol%), NaOH, DCM, H_2O_2 (33 %), 1h, rt, **c:** TBAHS (20 mol%) and NaOH, H_2O_2 (33 %), 30 min, rt.*

was present in the reaction mixture. The IR spectrum showed (C=O) stretching around 1670–1940 cm^{-1} depending on the assay and strong CO-O stretching absorption *ca*. 1130 cm^{-1}. After extracting the reaction mixture, no product was found once evaporated under reduced pressure. ^{1}H and ^{13}C NMR spectra of the empty RB flask made us suggest that the formed product was volatile since some starting material and decomposed product was found in NMR spectra.

According to the literature[54], [55], aromatic nitriles are more stable and can be converted to the corresponding amide in better yields than the aliphatic nitriles. This is mainly due to electron delocalization, which makes cyano carbon undergo the addition reaction faster. On the contrary, the reaction rate is slow at the first step and fast at the second in case of aliphatic nitriles and therefore the reaction can lead to formation of carboxylic acids. Methods for hydration of aliphatic nitriles usually involve the use of metals[56]–[58], surfactants[59] or transition metal-free catalyst as tetrabutylammonium hydroxide (TBAH)[60].

Due to the limited time, other reaction conditions were not assayed with the PEG nitrile **11**. However, we suggest that other approaches should be considered to synthesize **12** *e.g.* starting with acryloamide and DEG to obtain the final ligand on focus by substitution reaction with propargyl bromide and OH functional group[13], [61].

6. CONCLUSION

The synthesis of new 4-ethynylaniline derivatives containing water-soluble phosphane (PTA and DAPTA) or hydrophobic tri-1-naphthylphosphine ligand in second coordinative position of the metal atom were synthesized successfully and employed in molecular recognition studies with L-Glu and polyQ. The results are interesting in sense that both of

the guest molecules (L-Glu and polyQ) show interaction with their hosts. The binding mode is stronger in case of polyQ (possible due to a cooperative effect of the coordination of different gold(I) monomers to the same polyQ) and shows blue shifting in absorption spectra together with induced higher energy luminescence. Au···Au contacts are clearly affected by the interaction with polyQ possibly due to closer packing face to face into H-aggregates.

On the other hand, the binding with L-Glu resulted in fluorescence quenching together with lower absorptivity. According to the ^{1}H NMR studies, the binding mode is moderate in the case of **3** and **4** and involves both the phosphane as well as the 4-ethynylaniline moieties. The optical microscopy and DLS experiments also verified that the gold(I) complexes form large and complex cross-linked fibers with L-Glu and polyQ, when the guests alone assemble in spherical shapes and fibrillar structures. The size of the aggregates depend on the guest molecule so that in case of polyQ the host-guest systems were bigger and fibers up to 3 mm were observed in dried samples, by optical microscopy.

Furthermore, the photophysical properties of the synthesized complexes depend on the phosphane ligand. The complex **5** showed rich luminescence in solution due to three light absorbing naphthyl units. In case of **3** and **4**, the organic ligand was responsible for the luminescence. However, the acetyl units in DAPTA may have an influence on the intermolecular interactions as well as on dissolving ability in water and therefore affect positively on the resulting emission properties.

Au···Au contacts play a key role in the aggregation, which was inferred from the absorption spectra of **3** and **4** giving rise to long wavelength tail possibly originating from $\sigma^*_{Au\cdots Au} - \pi^*$ transition. In addition, information obtained from the variable temperature ^{1}H NMR experiments of **3** indicates that the Gibbs free energy change *ca.* -18 kJ/mol is close to our previous studies with related compounds and therefore supports the existence of short Au···Au distances. The driving force for the aggregation in case of **3** is clearly entropy rather than enthalpy. However, the aggregation depends greatly on the used solvent system and result in different kinds of aggregates.

Insight to synthesis of PEG amide was gained through several syntheses in different reaction conditions. Aliphatic nitriles tend to be a challenging outset for the hydrolysis reaction due to rapid formation of carboxylic acids. However, the work in this part will be continued with the information gained herein.

REFERENCES

[1] H. Schmidbaur *et al., Chem. Soc. Rev.*, **1995**, *24*(6), 391.

[2] V. W.-W. Yam and E. C.-C. Cheng, *Photochemistry and Photophysics of Coordination Compounds II*, Springer, **2007**, *281*, 269–309.

[3] H. Schmidbaur, *Gold Bull.,* **2000**, *33*(1), 3–10.

[4] J. W. Steed and J. L. Atwood, *Supramolecular Chemistry*, 2nd ed., Wiley, **2009**.

[5] M.-O. M. Piepenbrock, G. O. Lloyd, N. Clarke and J. W. Steed, *Chem. Rev*., **2010**, *110*(4), 1960–2004.

[6] A. Y.-Y. Tam and V. W.-W. Yam, Chem. *Soc. Rev*., **2013**, *42*(4), 1540.

[7] E. Aguiló *et al*., *Dalton Trans*., **2016**, *45*(17), 7328–7339.

[8] J. Lima and L. Rodríguez, *Inorganics*, **2014**, *3*(1), 1–18.

[9] M. D. Segarra-Maset, V. J. Nebot, J. F. Miravet and B. Escuder, *Chem. Soc. Rev*., **2013**, *42*(17), 7086–7098.

[10]C. Po, A. Y.-Y. Tam and V. W.-W. Yam, *Chem. Sci*., **2014**, *5*(7), 2688.

[11]J. C. Lima and L. Rodríguez, *Chem. Soc. Rev*., **2011**, *40*(11), 5442.

[12]C. Nardon, N. Pettenuzzo and D. Fregona, Curr. *Med. Chem.*, **2016**, *23*(29)

[13]R. Gavara, E. Aguiló, J. Schur, J. Llorca, I. Ott and L. Rodríguez, *Inorganica Chim. Acta*, **2016**, *446*, 189–197.

[14]J. Arcau *et al*., *Dalton Trans*., **2014**, *43*(11), 4426–4436.

[15]K. M. Ruff, S. J. Khan and R. V. Pappu, *Biophys. J*., **2014**,*107*(5),1226–1235.

[16]C. A. Ross, *Neuron*, **2002**, *35*(5), 819–822.

[17]H. Y. Zoghbi and H. T. Orr, *Annu. Rev. Neurosci*., **2000**, *23*, 217–247.

[18]A. D. Phillips, L. Gonsalvi, A. Romerosa, F. Vizza and M. Peruzzini, Coord. *Chem. Rev.*, **2004**, *248*, 955–993.

[19]S. H. Jung, J. Jeon, H. Kim, J. Jaworski and J. H. Jung, *J. Am. Chem. Soc.*, **2014**, *136*(17), 6446–6452.

[20]G. Hogarth and M. M. Álvarez-Falcón, *Inorganica Chim. Acta*, **2005**, *358*(5), 1386–1392.

[21]A. Muller, S. Otto and A. Roodt, Dalton Trans., **2008**, 650–657.

[22]E. Vergara *et al*., *Eur. J. Inorg. Chem*., **2007**, *2007*(18), 2926–2933.

[23]S. K. Schneider, W. A. Herrmann and E. Herdtweck, *Zeitschrift für Anorg. und Allg. Chemie,* **2003**, *629*(1213), 2363–2370.

[24]D.-A. Rosca, J. A. Wright and M. Bochmann, *Dalton Trans*., **2015**, *44*(48), 20785–20807.

[25]E. Atrián-Blasco, S. Gascón, M. J. Rodríguez-Yoldi, M. Laguna and E. Cerrada, *Eur. J. Inorg. Chem*., **2016**, *2016*(17), 2791–2803.

[26]L. L. Shevchenko*, Russ. Chem. Rev*., **1963**, *32*(4), 201–207.

[27]A. J. Moro *et al*., *Org. Biomol. Chem*., **2015**, *13*(7), 2026–2033.

[28]L. Rodríguez, M. Ferrer, R. Crehuet, J. Anglada and J. C. Lima, *Inorg. Chem*., **2012**, *51*(14), 7636–7641.

[29]E. Aguiló, R Gavara, J. C. Lima, J. Llorca and L. Rodríguez, *J. Mater. Chem. C*, **2013**, *1*(35), 5538.

[30]R. Gavara, J. Llorca, J. C. Lima and L. Rodríguez, *Chem. Commun.*, **2013**, *49*(1), 72–74.

[31]M. Ferrer *et al., Eur. J. Inorg. Chem*., **2008**, *2008*(18), 2899–2909.

[32]T. E. Müller *et al*., *J. Organomet. Chem*., **1994**, *484*(1–2), 209–224.

[33]E. Hobbollahi, M. List, G. Redhammer, M. Zabel and U. Monkowius, *Inorg. Chem. Comm.*, **2016**, *65*, 24–27.

[34]H. de la Riva *et al*., *Inorg. Chem*., **2006**, *45*(4), 1418–1420.

[35]V. W.-W. Yam *et al*., *Chem. Soc. Rev*., **2008**, *37*(9), 1806.

[36]C. E. Wayne and R. P. Wayne, *Photochemistry*, Oxford University Press Inc., **1996**.

[37]V. W.-W. Yam, K.-L. Cheung, S.-K. Yip and K.-K. Cheung, *J. Organomet. Chem.*, **2003**, *681*(1), 196–209.

[38]H.-Y. Chao *et al*., *J. Am. Chem. Soc*., **2002**, *124*(49), 14696–14706.

[39]R. Gavara, J. C. Lima and L. Rodríguez, *Photochem. Photobiol. Sci.*, **2016**, *15*(5), 635–643.

[40]U. Rösch, S. Yao, R. Wortmann and F. Würthner, *Angew. Chemie*, **2006**, *118*(42), 7184–7188.

[41]S. Ghosh, X.-Q. Li, V. Stepanenko and F. Würthner, *Chem. - A Eur. J.*, **2008**, *14*(36), 11343–11357.

[42]A. Vitalis, X. Wang and R. V. Pappu, *Biophys. J*., **2007**, *93*(6), 1923–1937.

[43]L.-N. Ji, X.-H. Zou and J.-G. Liu, *Coord. Chem. Rev*., **2001**, *216–217*, 513–536.

[44]P. Zhao *et al., Spectrochim. Acta Part A Mol. Biomol. Spectrosc*., **2015**, *137*, 227–235.

[45]R. Gavara, E. Aguiló, C. Fonseca Guerra, L. Rodríguez and J. C. Lima, *Inorg. Chem*., **2015**, *54*(11), 5195–5203.

[46]N. Ponnuswamy, G. D. Pantos, M. M. J. Smulders and J. K. M. Sanders, *J. Am. Chem. Soc*., **2012**, *134*(1), 566–573.

[47]P. Jonkheijm *et al*., *J. Am. Chem. Soc,* **2003**, *125*(51), 15941–15949.

[48]M. M. J. Smulders *et al*., *Chem. Pub. Soc*., **2010**, *16*(1), 362–367.

[49]K. Tambara, J.-C. Olsen, D. E. Hansen and G. D. Pantos, *Org. Biomol. Chem*., **2014**, *12*(4), 607–614.

[50]J. Shen *et al., Acta Pharmacol. Sin*., **2013**, *34*(3), 441–452.

[51]S. Cacchi, D. Misiti and F. La Torre, *Synthesis*, **1980**, *3*, 243–244.

[52]J. E. McIsaac, R. E. Ball and E. J. Behrman, *J. Org. Chem*., **1971**, *36*(20), 3048–3050.

[53]C. Bolchi, E. Valoti, V. Straniero, P. Ruggeri and M. Pallavicini, *J. Org. Chem.*, **2014**, *79*(14), 6732–6737.

[54]T. E. Schmid et al., *Catal. Sci. Technol*., **2015**, *5*(5), 2865–2868.

[55]R. S. Varma and K. P. Naicker, *Org. Lett*., **1999**, *1*(2), 189–192.

[56]K. Yamaguchi, M. Matsushita and N. Mizuno, *Angew. Chemie*, **2004**, *116*(12), 1602–1606.

[57]P. Marcé, J. Lynch, A. J. Blacker, and J. M. J. Williams, *Chem. Commun*., **2016**, *52*(7), 1436–1438.

[58]V. Cadierno, J. Francos and J. Gimeno, *Chem. - A Eur. J.*, **2008**, *14*(22), 6601–6605.

[59]L. Brinchi, L. Chiavini, L. Goracci, P. Di Profio and R. Germani, *Lett. Org. Chem.,* **2009**, *6*, 175–179.

[60]H. Veisi *et al., RSC Adv*., **2015**, *5*(9), 6365–6371.

[61]J. Arcau *et al., Dalton Trans*., **2014,** *43*(11), 4426–4436.

APPENDIX

Supplementary Information. Supplementary data associated with this Master's thesis can be found in additional Supplementary Information Appendix.

UNIVERSITY OF JYVÄSKYLÄ
Department of Chemistry

Supramolecular systems based on gold(I) derivatives. Molecular recognition of L-glutamine and polyQ.

Supplementary Information

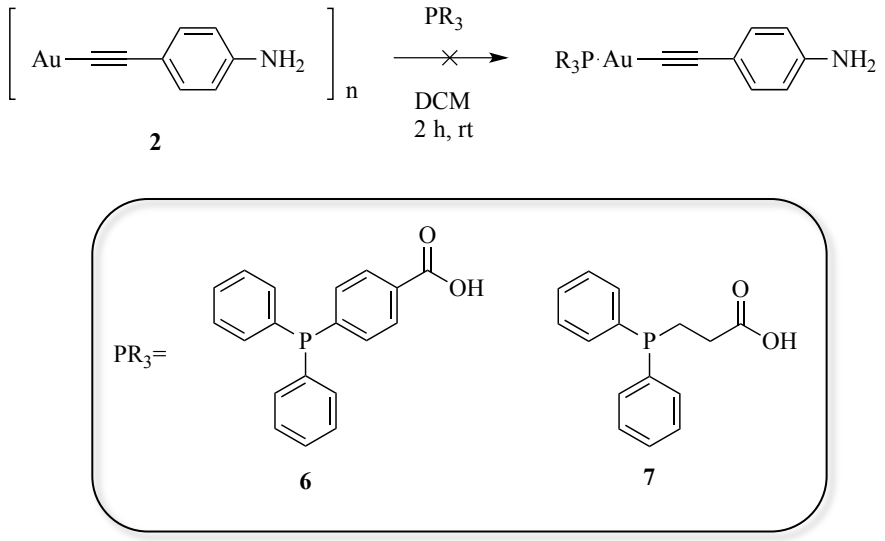

Scheme. S1. *Synthesis of [Au(4-ethynylaniline)(PR_3)] (PR_3= 4-(diphenylphosphanyl)benzoic acid **6**; 3-(diphenylphosphanyl)propanoic acid **7**.*

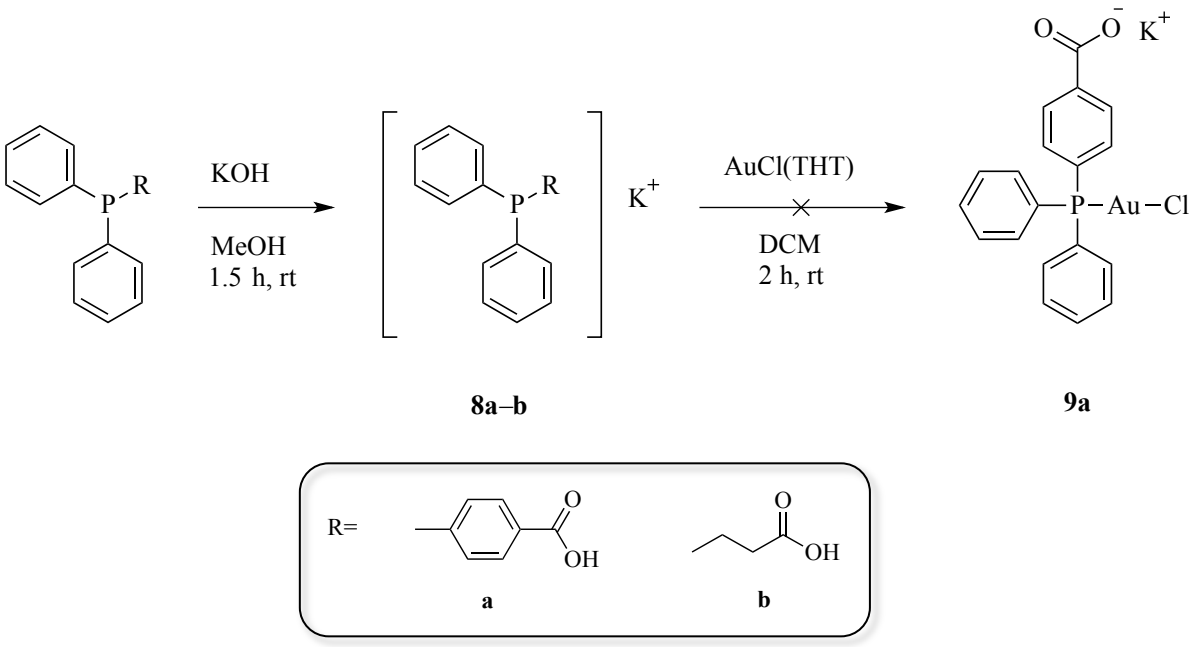

Scheme S2. *Synthesis of phosphine salt **8a**–**b** and anionic [AuCl(4-(diphenylphosphanyl)benzoic acid)] **9a**.*

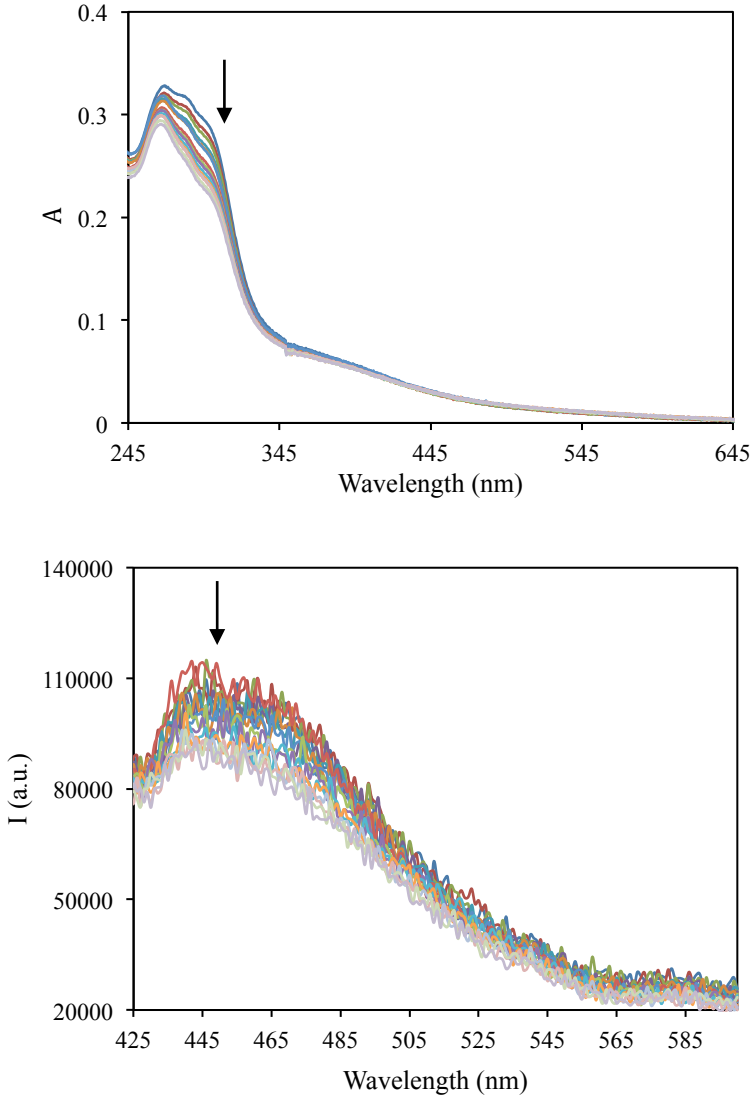

Fig. S1. *Absorption (top) and emission spectrum (bottom) (λ_{exc}=330 nm) of* ***3*** *at 2×10^{-5} M concentration in water upon addition of L-Glu. Arrows indicate increasing L-Glu concentration.*

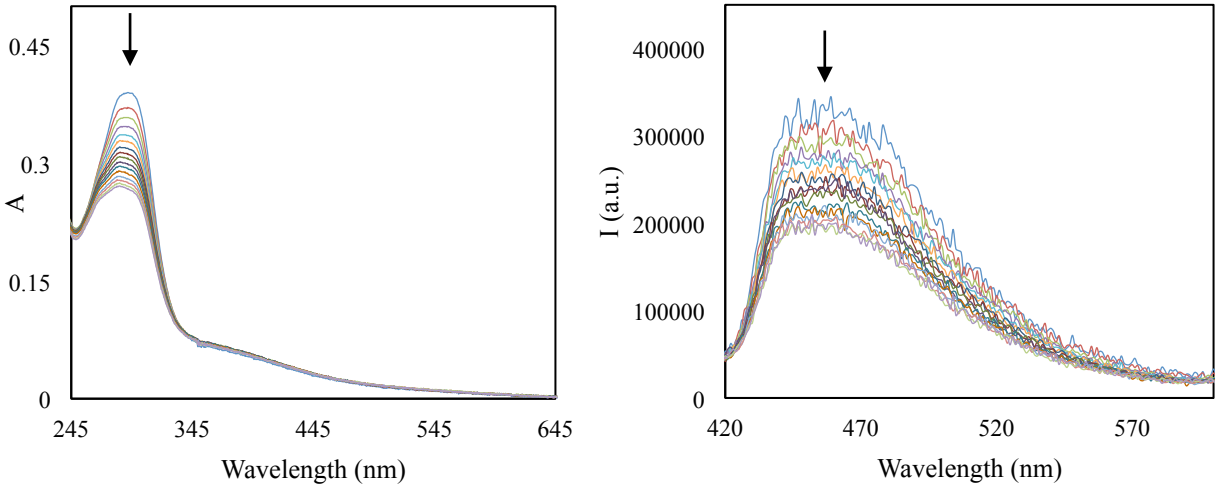

Fig. S2. *Absorption (left) and emission spectrum (right) (λ_{exc}=318 nm) of **4** at 2×10^{-5} M concentration in water upon addition of L-Glu. Arrows indicate increasing L-Glu concentration.*

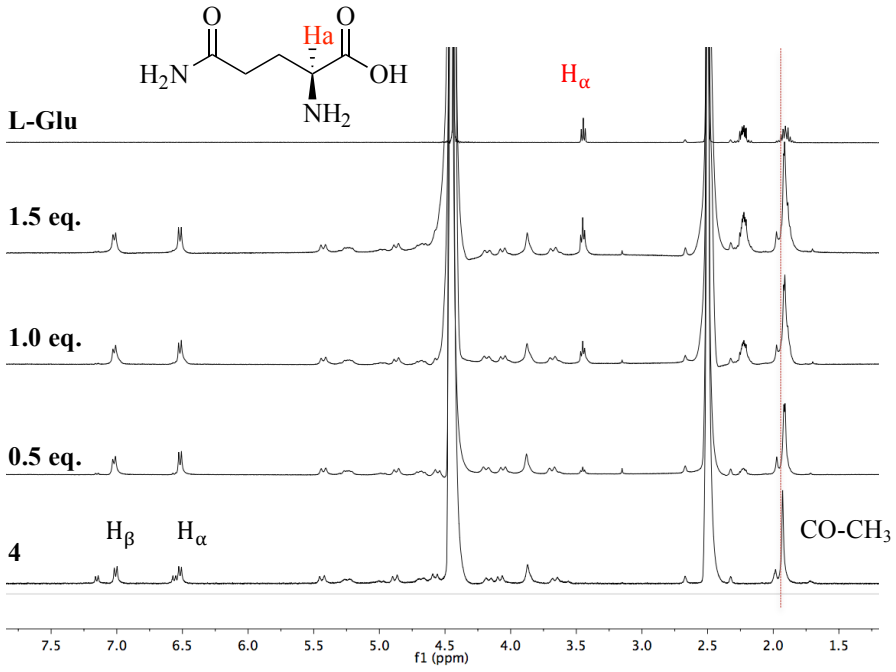

Fig. S3. *^{1}H NMR spectrum of **4**, L-Glu and **4** with 0.5, 1.0 and 1.5 eq. of L-Glu in D_2O:DMSO–d_6 at ca. 2×10^{-4} M concentration.*

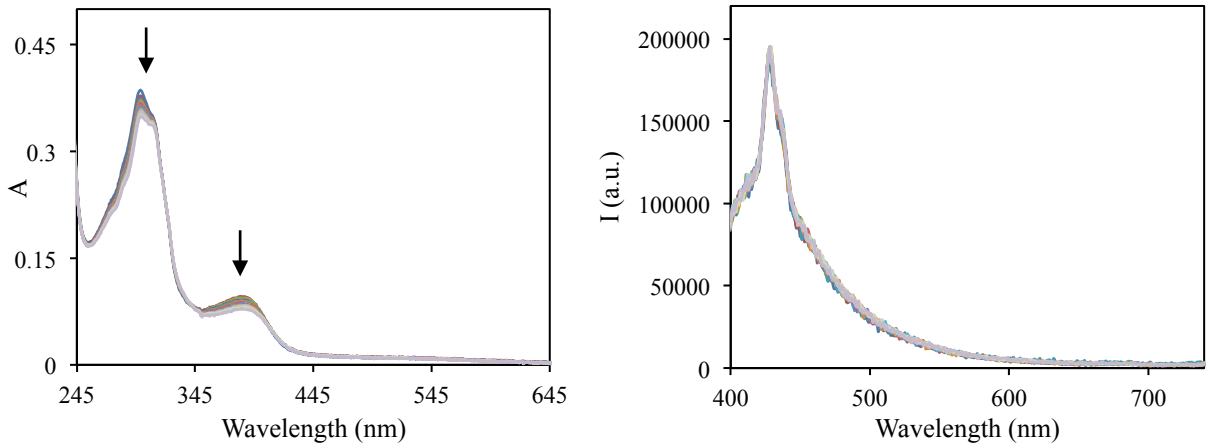

Fig. S4. *Absorption (left) and emission spectrum (right) (λ_{exc}=380 nm) of* ***5*** *at 10^{-5} M concentration in 1:1 THF:H_2O mixture upon addition of L-Glu. Arrows indicate increasing L-Glu concentration.*

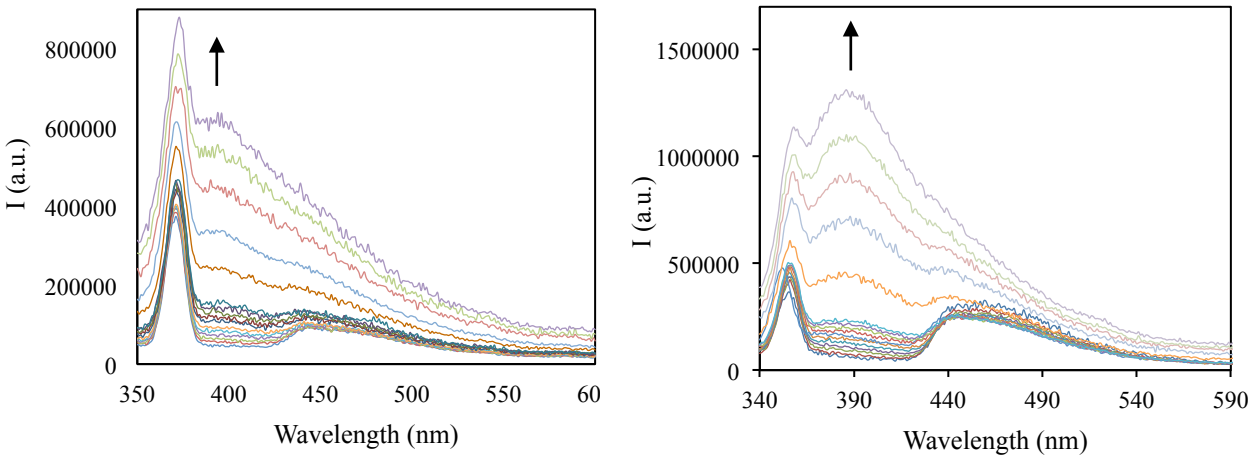

Fig. S5*. Emission spectrum of* ***3*** *(λ_{exc}=330 nm, left) and* ***4*** *(λ_{exc}=318 nm, right) at 2×10^{-5} M concentration in water. Arrows indicate increasing polyQ concentration.*

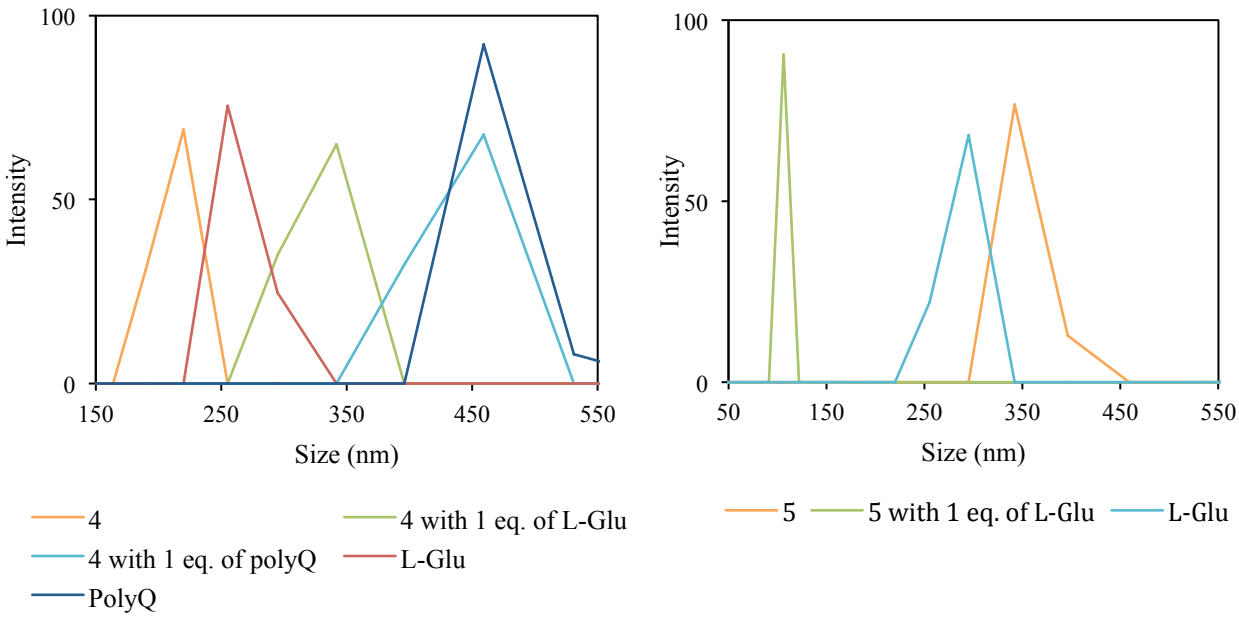

Fig. S6. *Left: size distribution of complex **4** at 2×10^{-5} M concentration with 1 eq. of polyQ and L-Glu and the guest molecules and the complex **4** alone in water. Right: size distribution of complex **5** at 10^{-5} M concentration with 1 eq. of L-Glu and the guest molecule and the complex **5** alone in 1:1 THF:H_2O mixture.*

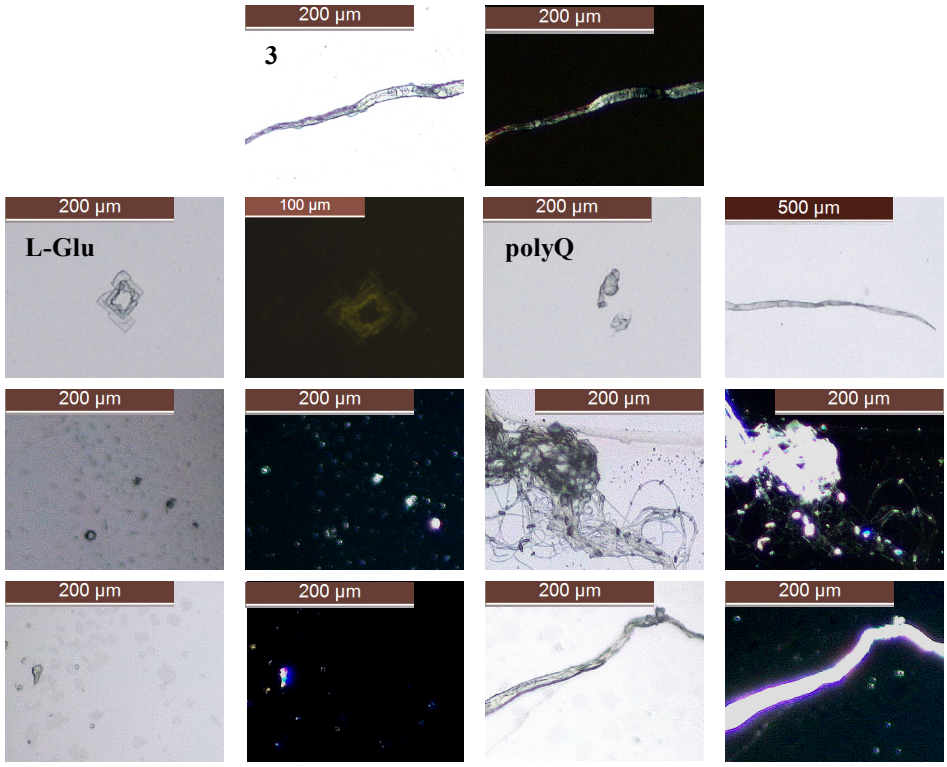

Fig S7. *Optical microscopy images with optical and polarized light of fibers of **3** (1st row), L-Glu and polyQ (2nd row), spherical aggregates and cross-linked fibers of **3** with L-Glu (3rd row) and polyQ (4th row).*

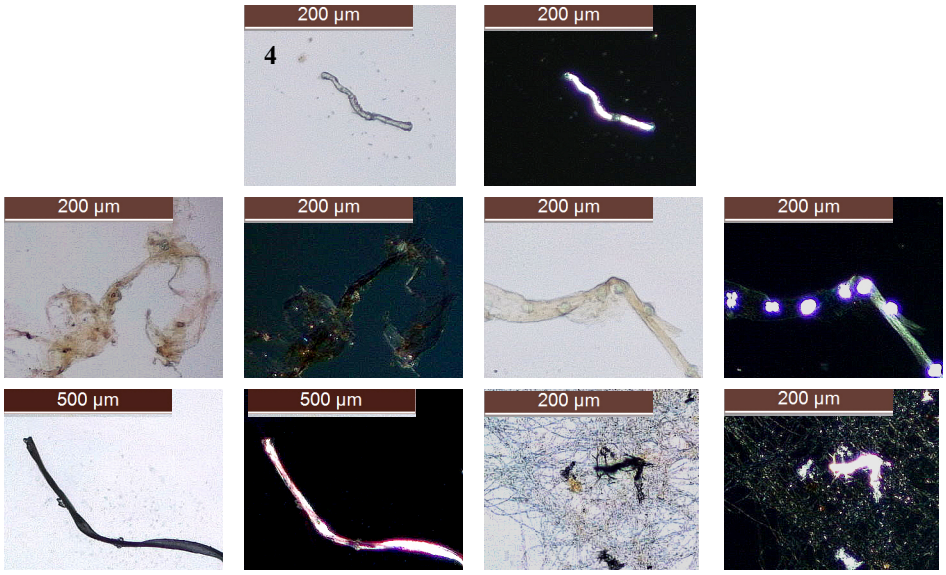

Fig S8. *Optical microscopy images with optical and polarized light of compound* ***4*** *(1st row), cross-linked and long up to 3 mm fibers of* ***4*** *with L-Glu (2nd row) and polyQ (3rd row).*

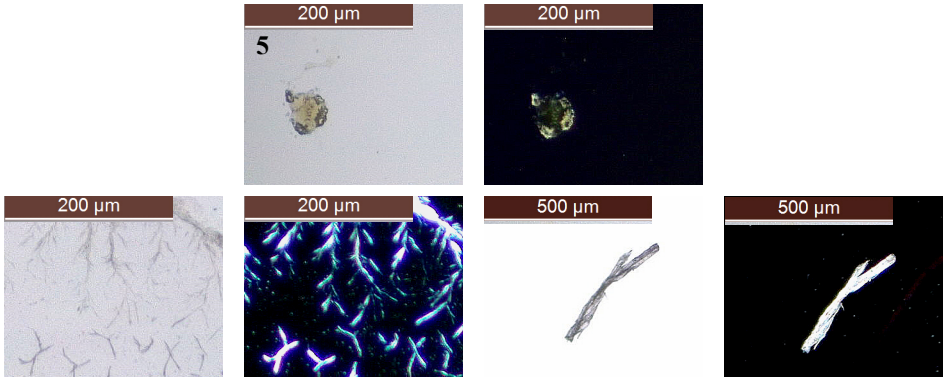

Fig S9. *Optical microscopy images with optical and polarized light of the complex* ***5*** *(top row) and cross-linked and long up to 1 mm fibers of* ***5*** *with L-Glu (bottow row).*

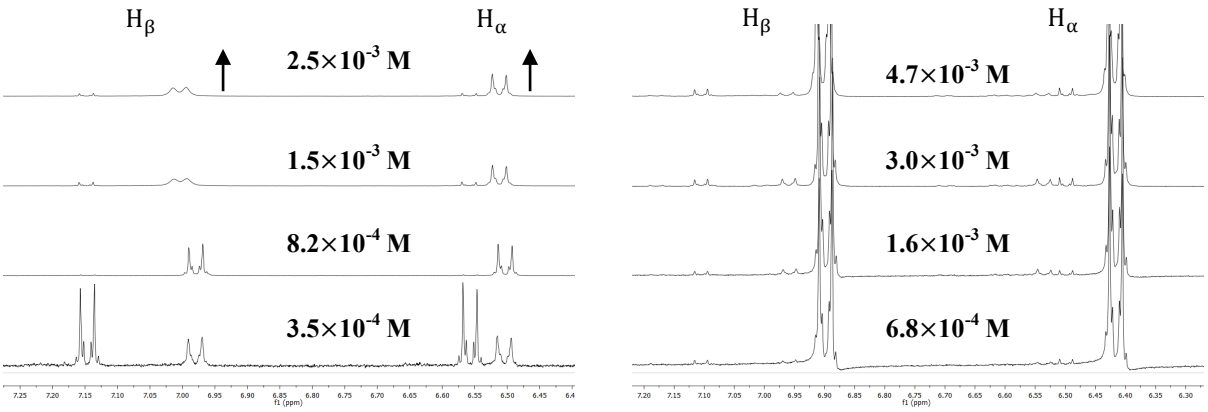

Fig. S10. *^{1}H NMR spectrum of **3** at various concentrations in 1:1 D_2O:DMSO–d_6 mixture (left) and in DMSO–d_6 (right) at 298 K.*

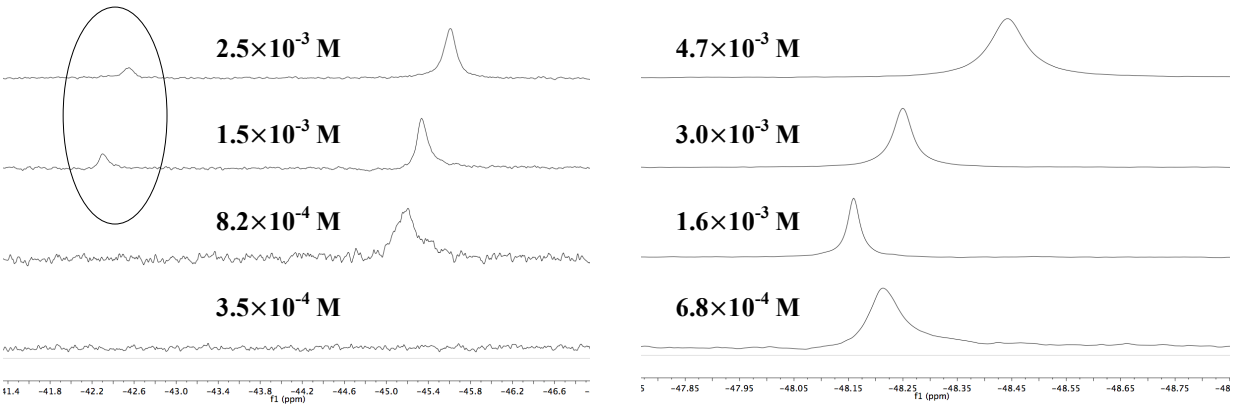

Fig. S11. *^{31}P NMR spectrum of **3** at various concentrations in D_2O:DMSO–d_6 mixture (left) and in DMSO–d_6 (right) at 298 K.*

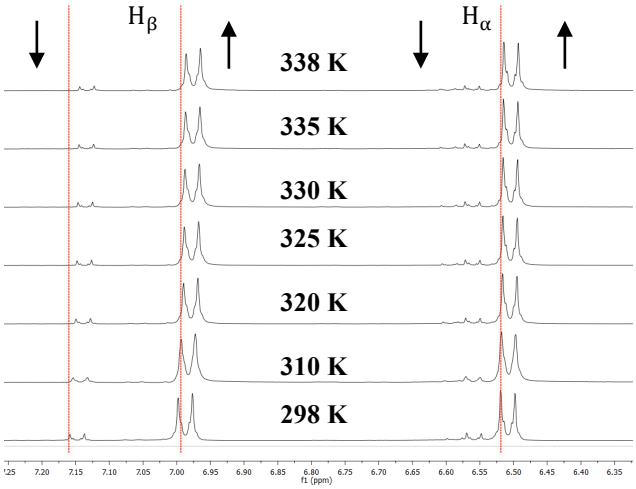

Fig. S12. *^{1}H NMR of **3** at 2×10^{-3} M concentration in 1:1 D_2O:DMSO–d_6 mixture at different temperatures. Arrows indicate the variation in integration.*

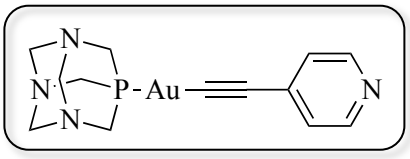

Fig. S13. *Related gold(I) alkynyl complex, [Au(C≡CC_5H_4N)(PTA)].*

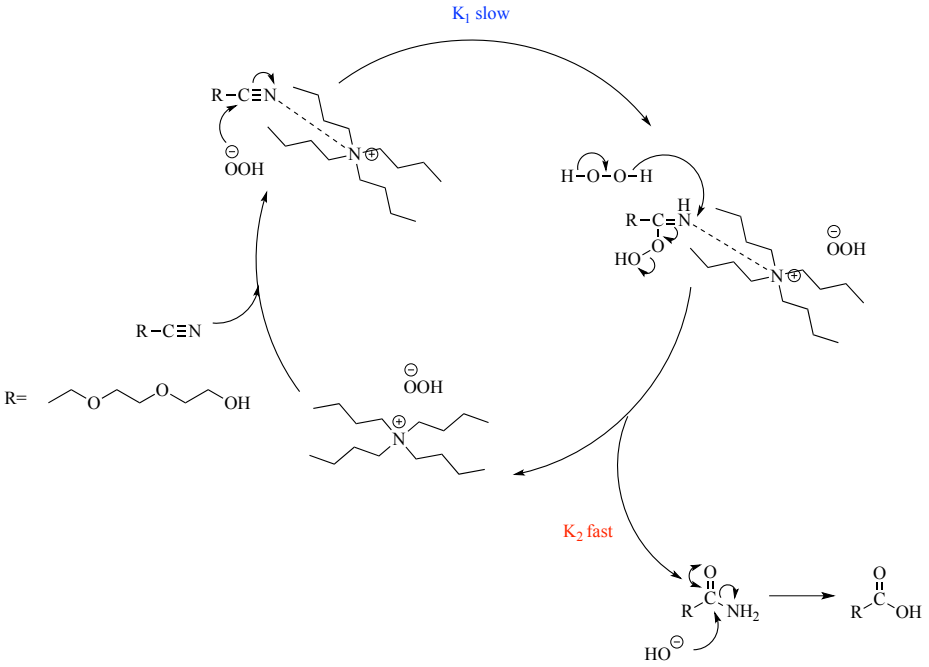

Fig. S14. *Proposed reaction mechanism of aliphatic nitrile and amide synthesis.*